Salinity and relative sea level rise in Heuningnes river South Africa

A field based Delft3D study

G.J. van der Ende

30-6-2015

WEM University of Twente
ITC University of Twente.
University of the Western Cape

PREFACE

First of all my gratitude goes out to my supervisors Denie Augustijn and Chris Mannaerts who both added a tremendous value to my graduation process. I am very happy with the trust and freedom that I have been given, so as to engineer this project into something I can satisfied with.

I am also considering myself lucky to have had access to the minds of Bas Borsje and Erik Horstman, who both found the time to think about the modeling problems I encountered, and were happy to share their experience with me.

The field campaign is one which would have been impossible and unlikable without the assistance of the University of the Western Cape. Dominic Mazvimavi has given me solid advise, knowing local circumstances. Also Michael Grenfell was a great asset, helping me out in the early stages of modeling, and Lewis Jonker allowing me access to some of the essential equipment which was used to acquire all data. Ultimate 'McGyvers' of the equipment and field-tips were Shamiel and Evan helping me out with lots of practical and crucial issues.

Of course I would also like to thank Mandy Carolissen for her support and advise in the field. It was always nice when there was a house with UWC students to come home to after a long day in the field.

Perhaps most importantly I would like to thank the local residents of Heuningnes river catchment for allowing me access to their land and waters, and in particular Pieter Albertyn, Johannes Uys, Michael van Breda and De Mond nature reserve manager Thulani Ndlovu. Talking to these fine men has given me great insight into the river system, as well as the present issues from a local perspective.

Finally I would like to thank Audrey Tollens for transferring her South Africa enthusiasm on to me, and allowing me off my leash for 3 months straight.

INDEX

Preface 1
1. Introduction 4
1.1 General introduction 4
1.2 Problem description 5
1.3 Research questions 5
2. Description of the study area 7
2.1 Catchment area 7
2.2 Tides 8
2.3 Discharge 9
2.4 Shape 9
2.5 Winds 10
2.6 Salinity 12
2.7 Relative sea level rise 13
3. Methods and Equipment 14
3.1 Introduction 14
3.2 Salinity and water levels 14
3.3 Bathymetry 17
3.3.1 Equipment 17
3.3.2 River width 18
3.3.3 Sampling method for depth data 19
3.3.4 Sonar head offset and tide correction 21
3.4 Discharge 22
3.5 Delft3D 23
3.6 Salt intrusion in literature 24
4. Measurement results 27
4.1 Salinity and water levels 27
4.2 Bathymetry 30
4.3 Inflow at the upstream boundary 31
4.4 Discussion 32
Water level data 32
Salinity data 33
Bathymetrical data 34
Discharge data 35
4.5 Preliminary conclusions 36

5. Modeling 38
5.1 Objective 38
5.2 Model scenarios 38
5.3 Input data and calibration 39
5.3.1 Upstream BC: Discharge and salinity 39
5.3.2 Downstream BC: Water levels and salinity 39
5.3.3 Bathymetry 39
5.3.4 Initial conditions 40
5.3.5 Roughness 40
5.3.6 Other input parameters 41
5.4 Results 41
5.4.1 Calibration results 42
5.4.2 Future situation 43
5.4.3 Sensitivity analysis 46
5.5 Discussion 49
6. General discussion 51
7. Conclusions and Recommendations 53
7.1 Conclusions 53
7.2 Recommendations 54
8. Bibliography 55
Appendix A: Model sensitivity for roughness and turbulence parameters 58
Roughness 58
Eddy viscosity 58
Eddy diffusivity 59
Appendix B: Heuningnes river bathymetry 60
Appendix C: Water level and salinity data 61
Appendix D: Wind direction and wind speed forecasts 64

1. INTRODUCTION

1.1 GENERAL INTRODUCTION

One of the most complex and fascinating water related research is, of course arguably, being done in the area where the river meets the sea. This is not only because of the beauty of the area itself, but also because of the complexity that comes with it. Water moves forward, backward, up, down and laterally. Fresh water meets salt water, waves meet the coast and tides can travel tens of kilometer upstream. Many forces and factors are involved in shaping this area: wind, currents, waves, gravity as well as topography, rainfall, temperature, density and surely quite a few others. And even from this seemingly chaotic reality, regularities can be deducted, and predictions can be made.

The subject of study in this thesis is the Heuningnes river, located in the Western Cape Province of South Africa. The river falls under the Breede Water Management Area (WMA), which is the southernmost WMA of South Africa. Heuningnes river is born from the excess water of Soetendaalsvlei, the second largest lacustrine wetland in South Africa, and the water of Kars river. It then flows it's 15 km long path in southeast direction into the Indian ocean (Figure 1). The area is of great importance for its biodiversity, since extremely rare birds, fish and plants are found within the area (Cape Nature, 1998). The river however is not in its full natural state. In the early 20th century and before, the downstream river mouth used to be temporally closed when flow in the Heuningnes river was limited. Only during large floods the coast was breached and the connection with the Indian Ocean was established. This system however caused frequent inundations upstream and management of the river mouth was initiated at the beginning of the 20th century. The mouth was kept open permanently until 1973 when it was allowed to naturally close for a three year period. In 1976 it was reopened again and has been kept open since (Bickerton, 1984).

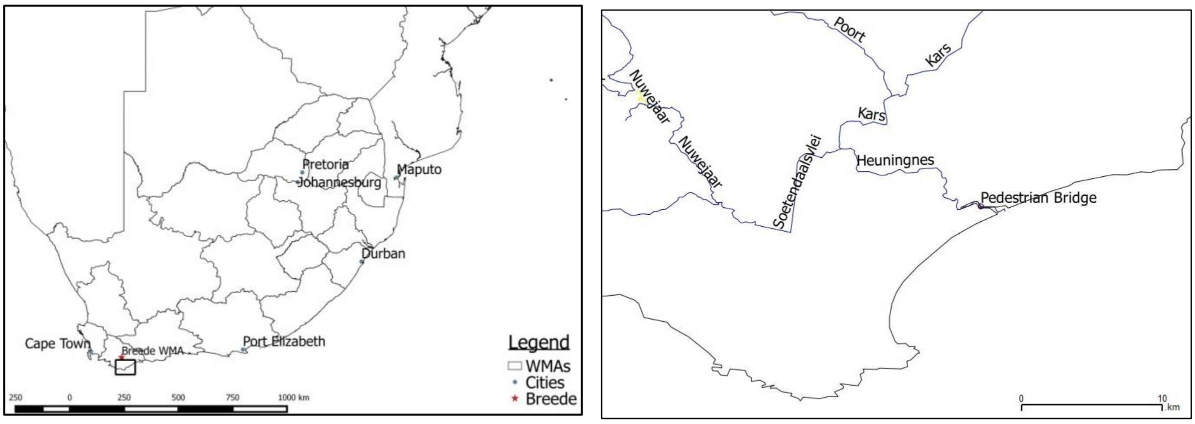

FIGURE 1.1: (LEFT) WMAS IN SOUTH AFRICA (DEPARTMENT OF WATER AFFAIRS AND SANITATION (DWAS)); (RIGHT)HEUNINGNES RIVER SYSTEM (DWAS).

1.2 Problem description

The current general state of the Heuningnes river is rated 'Good' in the 2011 State Of The River Report (DWAS, 2011). It describes a river which is in good health, scoring either 'Fair' or 'Good' in all categories. A direct pressing problem to the river's health is thus not the issue. However with such a vibrant river it is all the more important to monitor its development in order to anticipate possible future problems.

But also, there are more river related aspects than just river health itself. Currently much discussion is taking place on inundation risks of Heuningnes river. These inundations threaten the valuable agriculture lands in the area. One farmer mentions a 'loss' of 10% (some 400 hectares) of his land which is now only usable as grazing land, while previous generations were still able to use this land for more profitable crops. Up until now these inundation are reported to be dominated by fresh water (Pieter Albertyn, personal communication, January 2015).

With Heuningnes river flowing directly into the Indian Ocean, and relative sea level rise (RSLR) predictions being above average for South Africa, it is not hard to imagine possible future problems for the Heuningnes river catchment. It seems likely that Heuningnes river will become more saline in the future due to the elevated level of the ocean (HiLand Associates, 2009). This has a number of possible implications. Firstly, reflecting on the aspect of nature management in the Heuningnes river. Although a more saline river is not bad for nature by itself, it should be considered that for instance salt water fish will migrate further upstream, and in this case leaving the protected area downstream moving to the less protected areas upstream. This might result in an increase in illegal fishing on already threatened species (Thulani Silence Ndlovu, personal communication, January 2015). Secondly, inundations are likely to be more frequent due to higher sea water levels, which poses a problem for landowners and their crops. This may become ever more serious in case these inundations are not only freshwater, but become more saline as a consequence of these higher sea levels. Thirdly, it is currently still very unclear how far this salinity will move upstream under which circumstances, and how large the impact of RSLR will be on this issue. It has been reported that saline water has reached all the way into Soetendaalsvlei, which if happening more often, would have consequences for the nature in Soetendaalsvlei, as well as its potential use for irrigation.

1.3 Research questions

In order to give more clarification on the size and scope of the issues discussed, the following research question has been posed:

"*How is the current salinity profile formed under the different tidal conditions and discharge regimes in Heuningnes river, and to what extent will RSLR have an impact at the end of the 21st century on the salt concentrations along Heuningnes river?*"

This can be broken down into two sub questions:

1. *From where does salt in Heuningnes river originate and what does the spatial distribution look like as a result of different downstream water levels and discharge regimes?*
2. *What will the influence be of an increased relative sea level at the end of the 21st century on salt concentrations in Heuningnes river?*

This thesis should thus give answer to the question what the projected change in salt concentration will be along the river. Secondary effects like consequences for nature and farming which may result from future changes in salt concentrations will only be briefly mentioned.

In order to answer the research questions posed a field campaign will be organized to gather the necessary data. This data will already answer part of the research questions, but will also be used to set up a model. This model then answers the remaining part of the questions by simulating various tidal conditions, discharge regimes and RSLR.

The next chapter will start describing the study area using reports publicly available and observations from the field campaign. Chapter 3 will go into the methodology and equipment used to gather all the data in the field, as well as give a short description on the model used. This is then followed by a chapter describing the data gathered in the field campaign. Chapter 5 expands on modeling, the objective, set up, calibration and results, followed by a discussion on the modeling as well as the data limitations. Chapter 6 is a more general discussion, and finally a chapter on conclusions and recommendations is written.

2. Description of the study area

2.1 Catchment area

The study area falls within the larger Breede Water Management Area (WMA), see Figure 1.1. This area is located in the southernmost tip of the African continent. Then going to the south of this area we find Overberg East catchment which comprises 4128 km^2 and receives a mean annual precipitation of 428 mm. Potential evaporation is estimated at 1449 mm and average yearly runoff is estimated at only 24 mm (99 million m^3) (DWAS, 2011). Summers are generally hot and dry with temperatures of minimum 15 degrees to maximum 28 degrees Celsius, whereas the winters are rather wet with temperature between 6 and 17 degrees Celsius (Bickerton, 1984).

The area of the Heuningnes river catchment is estimated to be between 1185 and 1938 km^2 depending on which source is used. To the west of Heuningnes river, Soetendaalsvlei is located. This is a large wetland being fed by Nuwejaars river. The overflow of this wetland confluences with the Kars river a few kilometers further downstream forming Heuningnes river, see Figure 1.1. Total length from the point of confluence to the mouth is 15 km (Bickerton, 1984).

Figure 2.1: Soetendaalsvlei (top)(DWAS, 2011), Heuningnes river channel upstream (middle left), middle (middle right), downstream (bottom).

Heuningnes catchment is a very flat area. Based on in situ measurements, bed level elevation decreases only 1.7 to 4 meters when moving from 12 km upstream towards the river mouth. This would imply a slope of about 0.00014 to 0.00033. A more detailed bathymetry can be found in appendix B. This is also the reason why the area is so prone to flooding. In an effort to battle this problem the mouth of Heuningnes river has been kept open artificially for most of the time starting early in the 20th century, so that excess water can always be discharged towards the Indian Ocean. Despite these efforts flooding does still occur.

The flat surface makes it possible for a few interesting scenarios to unfold. Depending on which part of the catchment receives a lot of rain, Heuningnes river can flow in both directions. Not only because of tidal influence, which is measurable above the Heuningnes-Kars point of confluence, but also discharge from Kars has been reported to make Heuningnes flow in the upstream direction, towards Soetendaalsvlei (Pieter Albertyn & Johannes Uys, personal communication, January 2015).

Upstream in Heuningnes river, the river channel is relatively narrow and vegetated by reeds. Further downstream it becomes wider and reeds become more sparse. Even closer to the estuary mouth some sandbanks occur, and the channel becomes less well defined, see Figure 2.1.

Main land uses to be found in Overberg East catchment are dry land agriculture, nature and some vineyards. Most of the geology are Bokkeveld shale, responsible for the naturally saline water in the rivers (DWAS, 2011). More specifically, in the catchment of Heuningnes river we find 41% of the land covered by agriculture, mostly wheat, barley as well as dryland pastures (DEAT, 2001; Leeuwner *et al.*, 2003 in Cape Nature, 2005). Zooming in to the lands directly adjacent to Heuningnes river, farmers report to be planting predominantly barley, oats, canola, triticale and wintergrain.

2.2 TIDES

At the mouth of the Heuningnes, the semi-diurnal tide is dominant. Tidal range is limited and can be classified as micro tidal (<2 m). Tidal range at spring tide is 1.75 m. More details can be found in Table 2.1. Reference level used for the tidal data is unknown, however relative values do give interesting insight in the local circumstances.

TABLE 2.1: TIDAL DATA (CAPE NATURE, 1998).

Stage	Level [m]
Highest Astronomical Tide	2.42
Lowest Astronomical Tide	0.01
Mean High Water Springs	2.00
Mean Low Water Springs	0.25
Mean High Water Neaps	1.41
Mean Low Water Neaps	0.84
Mean Level	1.13

When moving into the river tidal effects are damped and water levels fluctuate slightly less than one meter. Water levels are observed slightly upstream of the river mouth for the months November, December and January of 2012 and can be found in appendix C. Tidal influence is reported to be up to 12 km upstream (HiLand Associates, 2009).

2.3 DISCHARGE

Discharge in Heuningnes river is characterized by its clear seasonal behavior. In the dry summers it can be virtually zero, while during winter large floods can occur. A recent flood was reported in April of 2005 when some 12.000 ha of farmland was inundated (Cape Nature, 2005).

Data on discharge in Heuningnes river is not largely available. Some numbers however have been produced in the past. Bickerton (1984) suggests a mean annual runoff of 78.3 million m^3, but also mentions 37.6 million m^3 as a more recent figure (Bickerton, 1984). This last number is also found in more recent reports (DWAS, 1998b in Cape Nature, 2005). Aside from being quite far apart, these numbers are also based on simulations, not measurements. For now we can only assume these data to be correct. Translation to monthly averages are also given in the same report showing a maximum (monthly averaged) discharge of 2.3 m^3/s in wet winter months, which declines to an average of almost zero in the dry summer months. In these calculations (extreme) events are thus averaged out.

The only measurements available have been produced by the University of the Western Cape (UWC) September 2014, where they found a discharge of 5 m^3/s. Based on measurements taken earlier in the year further upstream, UWC estimates the discharge in a wet month to be close to 17 m^3/s.

2.4 SHAPE

The shape of the river is diverse. When we move from downstream to upstream we find many bends near the outlet of the river, as well as further upstream.

The mouth of the river is a rather dynamic area. Exact location and depth of the mouth vary over time. For instance the river mouth has been reported to have a tendency to move 100 west and eastwards depending on hydrodynamics (Walsh, 1968 in Bickerton, 1984).

Also evidence of bend erosion can be found in the river. At one location a submerged concrete wall has been placed in the bend, to combat further erosion and protect a cottage which is standing close to the river.

When looking at the cross sectional shape of the river we find a clear difference between the upstream section and the downstream section. From Soetendaalsvlei until about 4 km before the mouth the river is formed by a relatively well distinguished channel, which in most cases is about 2 meters deep. The last 4 km of Heuningnes river are characterized by a more flat and wider channel where at some places during low tide, the river can be crossed while only going knee deep.

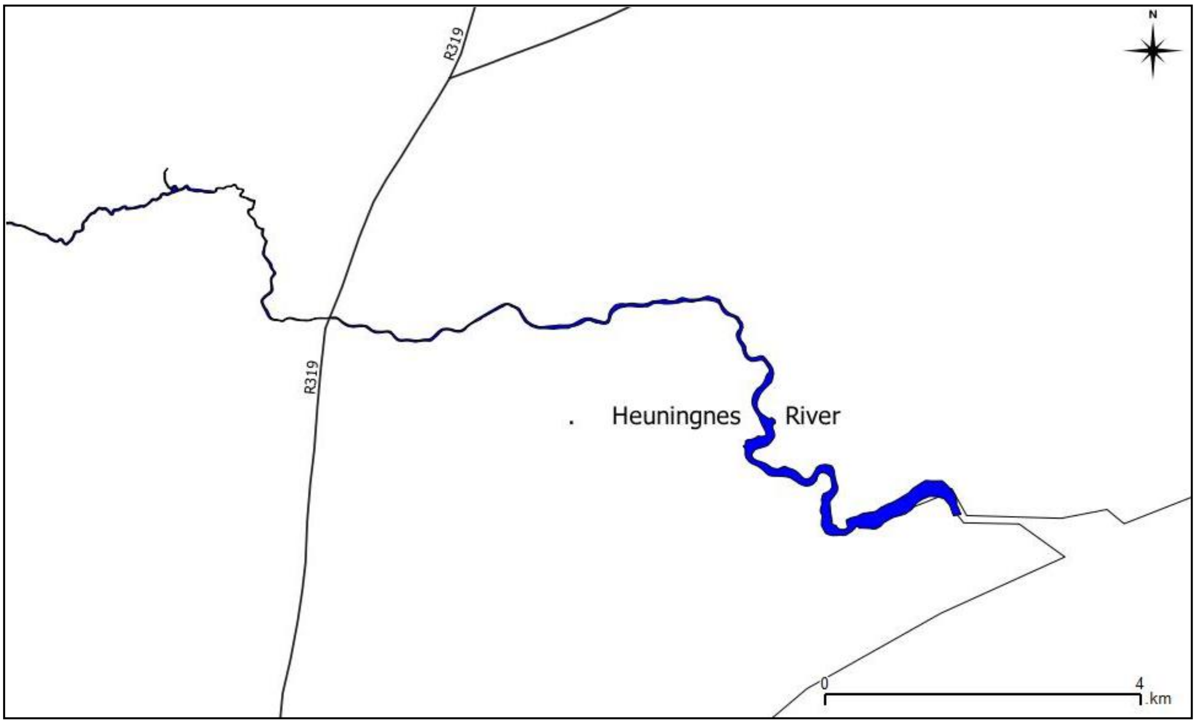

FIGURE 2.2: RIVER SHAPE (BASED ON GOOGLE EARTH, 2012).

2.5 WINDS

Dominant winds during spring and summer come from the south. It is reported that in spring 63% and in summer 62% of the time wind is southwest to southeast. Wind speeds are measured around 15 m/s. An overview taken from Bickerton 1984 can be found in Figure 2.3 (Bickerton based this data on rough data gained in personal communication). Wind speeds and direction forecasts for the period of field work can be found in appendix D.

Large parts of Heuningnes river is bordered by 1 meter high reeds, which are present year round. This protects the river from major influences of the wind. However when wind speed become relatively large, or the river becomes wider, wind influence may become significant. From experience on the river can be stated that a wind speed of about 15 m/s can produce waves with an amplitude of about 30 to 40 centimeters.

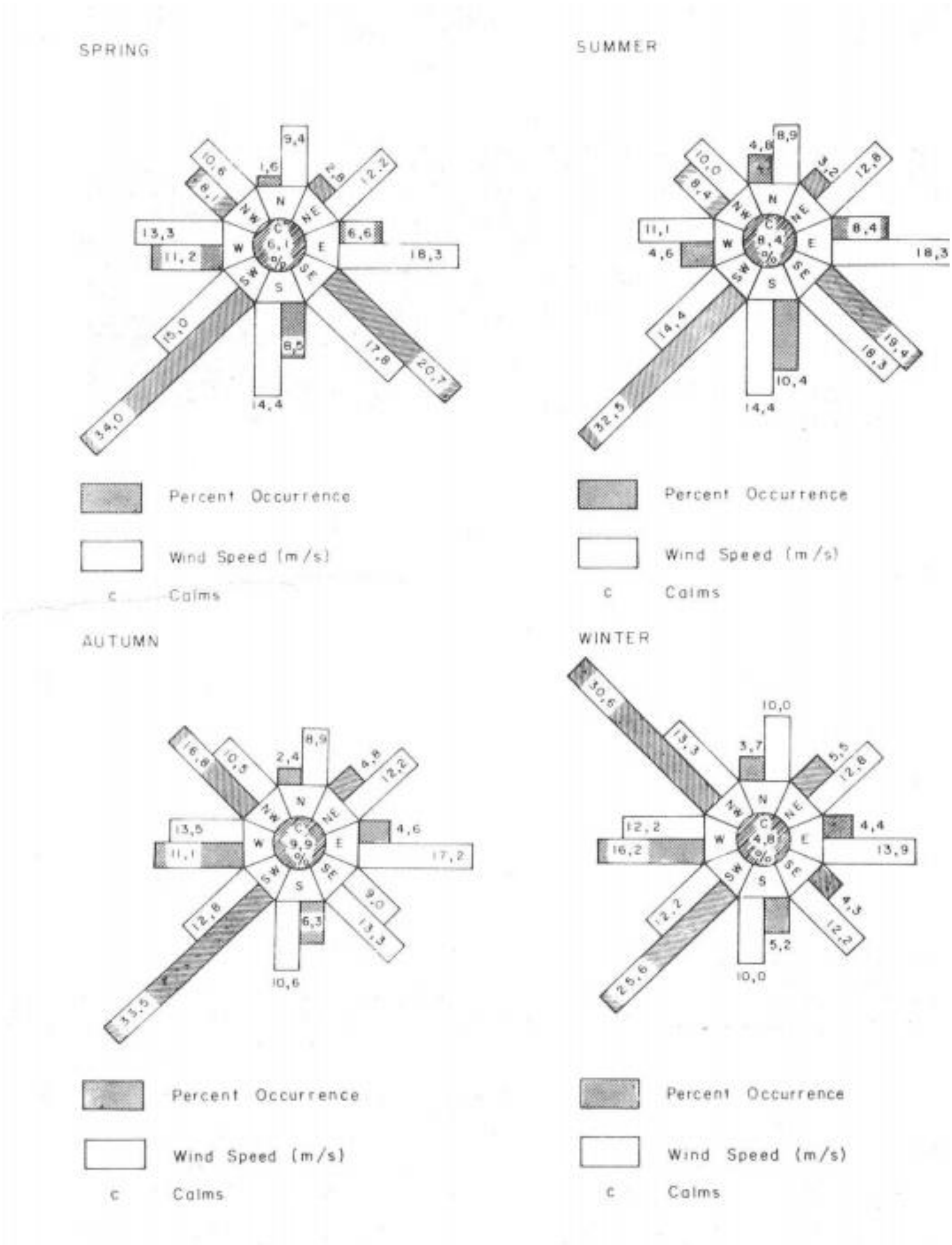

FIGURE 2.3: WIND SPEED AT MOSSELBAY 1976-1980 (Bickerton, 1984).

2.6 SALINITY

The salinity in Heuningnes river is determined by three sources (1) upstream salinity levels, (2) saline runoff from within Heuningnes catchment and (3) ocean water intrusion. Some measurements have been taken upstream which are shown in Table 2.2. The relative large values for these samples show the relative high natural salinity already present in the system and coming in from upstream of both tributaries Kars and Nuwejaars river. Much of this salinity is due to the geology in the catchment which can be seen in Figure 2.4. Malmbury group which consists predominantly of shale is usually associated with saline water. The Bokkeveld group which also consists mostly of shale is exceptionally saline, with groundwater EC of 2.7-5.6 ppt. Bredasdorp groups is associated with groundwater EC of less than 2 ppt (Cape Nature, 2005).

TABLE 2.2: SALINITY OF UPSTREAM LOCATIONS AND SOME OTHER WATER SYSTEMS FOR REFERENCE (VALUES CONVERTED FROM ELECTRICAL CONDUCTIVITY DATA USING(Lewis, 1980)).

Location	date of sample	Salinity [ppt]	Reference
Soetendaalsvlei	-	1.5 - 3.8	Toens 1998
Soetendaalsvlei	4-7-2013	2.43	DWAS
Kars	jan-98	1.41	Toens 1998
Kars	1966-1988	0.85	DWAS
Lower Rhine	1979-2004	0.2 - 0.4	(Friedrich & Pohlmann, 2009)
Ocean average	-	31	(Mizuno & Watanabe, 1998)
Fresh water	-	0.05 - 0.5	(Chapman 1996 in Campbell, 2009)

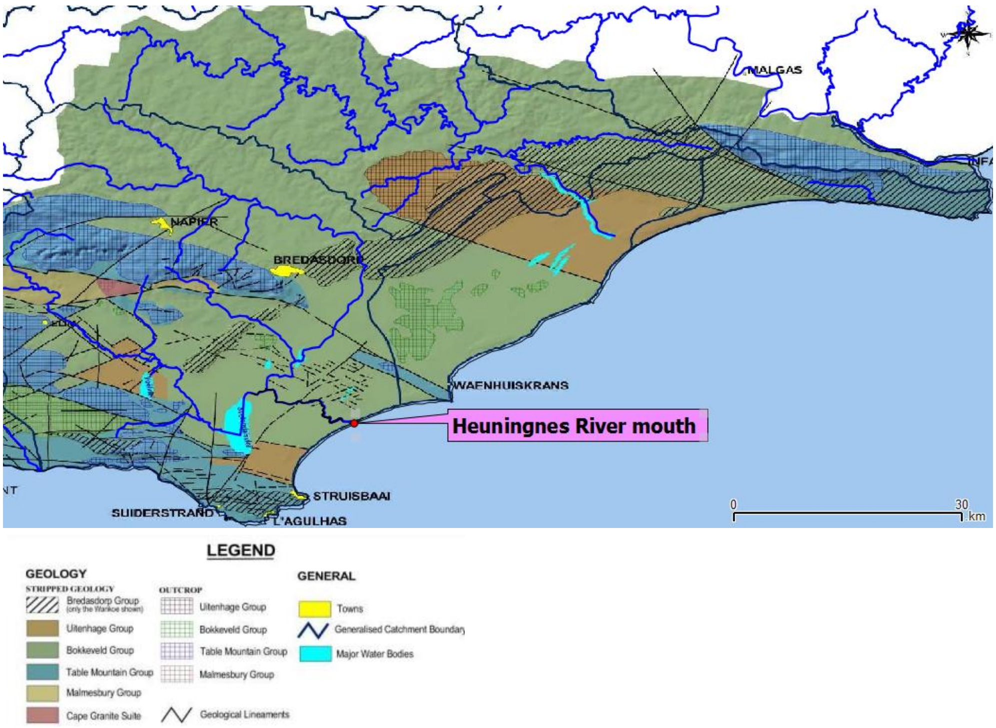

FIGURE 2.4: GEOLOGY BREEDE WMA AND SURROUNDING AREA.

2.7 RELATIVE SEA LEVEL RISE

In order to properly formulate the boundary conditions of the model, solid estimations of future sea level rise are needed. IPCC is doing valuable research into the area of relative sea level rise (RSLR). In the Fifth Assessment Report from the IPCC (AR5), it is stated that since the late Holocene, when sea level rise (SLR) is estimated in the order of tenths of millimeters per year, the rate of SLR has accelerated to almost 2 mm/year over the 20th century. These numbers are based on a combination of paleo sea level data and long tide gauge observations.

However it is not just the change in sea level which is of interest but the RSLR. Aside from absolute change in sea level this also includes processes that change the absolute level of the landmass.

Scholars have developed many different models all projecting global relative sea level change. In AR5 some 21 different models are shown all giving their own projections for RSLR on the globe. Again all these models can be run using different scenarios proposed by IPCC. Based on this comprehensive study IPCC concludes that it is virtually certain that sea levels will continue to rise during the 21st century.

The RSLR is not the same everywhere on the globe. Unfortunately South Africa lies in a zone which experiences a larger than average RSLR. Regional levels, based on data from 21 models, are depicted in Figure 2.5 for different Representative Concentration Pathways (RCP) scenarios. Differences in these scenarios are based on assumed concentrations of greenhouse gases in the atmosphere. Based on these data we find a RSLR at the South African coast between 0.4 and 0.7 meters by the end of the 21st century.

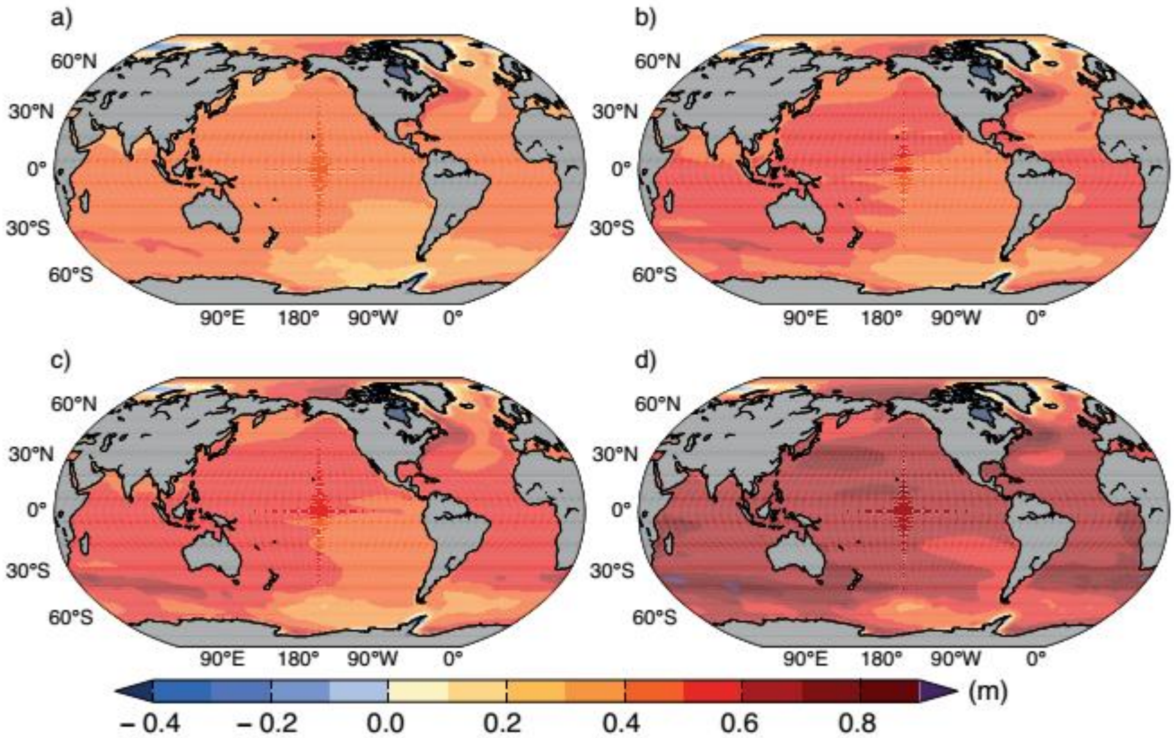

FIGURE 2.5: RELATIVE SEA LEVEL CHANGE FOR DIFFERENT (RCP) SCENARIOS BETWEEN 1986-2005 AND 2081-2100 (Church et al., 2013).

3. METHODS AND EQUIPMENT

3.1 INTRODUCTION

In this chapter an overview is given of the methods and equipment used in order to collect the data and answer the posed research questions. Descriptions and technical details on the various measuring devices used will be presented, as well as the limitations that come with the used devices. Also all reasoning behind the use of selected methods will be explained.

First data collection will be discussed, explaining the methods and practices used while gathering data in the field. This was done starting at the end of November 2014 until the end of January 2015. Final paragraph of this chapter will go into the model selected and the reasoning behind the model choice.

3.2 SALINITY AND WATER LEVELS

In order to be able to correct the bathymetrical survey described in 3.3, as well as for calibration and validation of the model, continuous water level data is needed at several locations in the river. Also continuous salinity measurements are needed for calibration and validation of the model. These measurements have to be taken at strategic locations in an effort to properly capture the variation in salinity which is expected to be moving up and downstream depending on the tide.

FIGURE 3.1: OTT CTD DIVER. THE PROBE IS ATTACHED TO A LONG CABLE WHICH ENDS WITH THE READER UNIT WHICH CAN BE BURIED NEXT TO THE RIVER.

Four OTT CTD divers were available for installation in the field (see Figure 3.1). These divers measure conductivity, temperature and depth at a user defined interval. The CTDs were programmed to observe data every 6 minutes. All conductivity measurements were internally corrected for temperature using Standard Method 2510. All CTDs have been installed in protective tubes which were perforated with large holes so that water would refresh easily in the tubes. These were subsequently attached with cable ties to a wooden pole which was driven into the river bed. Divers were thus floating vertically in the water at about 10 cm above the river bed. Resulting conductivity values in mS/cm were converted to practical salinity units (psu) using a method proposed in USGS guidelines report (Lewis, 1980 in Wagner et al. 2006), see equation 3.1. These units are nearly equivalent to part per thousand, and will in this thesis be referred to as such.

$$S = K_1 + (K_2 R^{0.5}) + (K_3 R) + (K_4 R^{1.5}) + (K_5 R^2) + (K_6 R^{2.5})$$

where

$$K_1 = 0.012$$

$$K_2 = -0.2174$$

$$K_3 = 25.3283$$

$$K_4 = 13.7714$$

$$K_5 = -6.4788$$

$$K_6 = 2.5842$$

and R is the specific conductance at 25 degrees Celsius.

FIGURE 3.2: CTD PROTECTIVE TUBE AND SUBMERGED ATTACHMENT POLE.

In an effort to find suitable locations for installing the CTDs, measurements along the river were taken starting at the R319 bridge and moving further downstream. Every approximately 800 meter measurements were taken alongside the river, in the middle of the river, as well as over the vertical column. This to determine if any form of stratification of salinity was present in the river. Based on these initial results locations for the first three CTDs were selected: CTD1, CTD2 and CTD3 (see Figure 3.3). CTD1 covers the salinity of the inflow into the model, while CTD2 and CTD3 observe the variation of salinity over time at their respective locations. After first analyses of the data produced by CTD1, 2 and 3 it was decided to add one location between CTD1 and CTD2, to be named CTD1.5. This because the river was likely to become more saline over time in summer due to the low rainfall, and the saline front might have moved even further upstream.

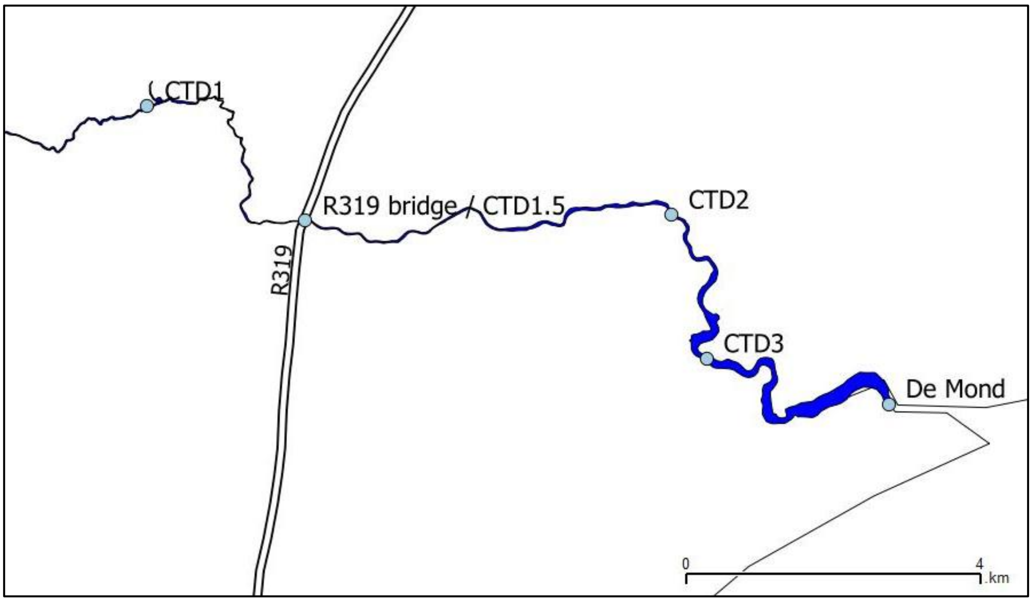

FIGURE 3.3: LOCATIONS CTDS.

Aside from the salinity data, the CTDs also produce depth data. But in order to be able to use this properly, the depth data should be converted in water level data by referencing them all to a fixed datum. Only then can they be used to properly correct the bathymetrical survey data which is to be discussed in 3.3. For this task centimeter accurate elevation measurements were needed, which have been done with specialized equipment owned by the Department of Agriculture (see Figure 3.4 left).

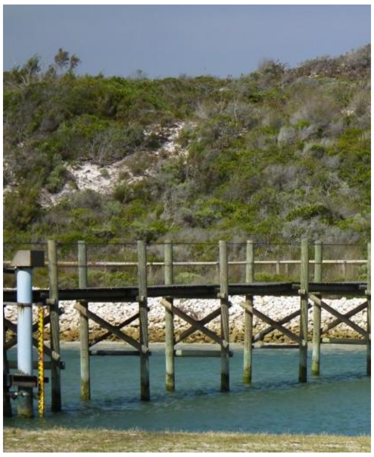

FIGURE 3.4:(LEFT)SURVEY TEAM DEPARTMENT OF AGRICULTURE, (RIGHT) DOWNSTREAM WATER LEVEL GAUGE DWAS.

In addition at the river mouth all the way downstream a water level logger was present (De Mond, Figure 3.3). This water level logger was, and quite likely still is, operated by the Department of Water Affairs and Sanitation (DWAS) producing water level data at a 12 minute interval. This data is to form the lower boundary condition of the model, as well as being used for bathymetrical data correction.

3.3 Bathymetry

In literature it is stated that the bathymetry plays a very important role in the behavior of the model. Drawing from experience with the to be used model Delft3D in other similar sized rivers in South Africa the goal is to create a bathymetry with an accuracy of at least 5-10 cm in terms of bed levels (Van Ballegooyen et al., 2004).

The equipment available for this task is listed in Table 3.1 below.

Table 3.1: Equipment for bathymetrical data acquisition.

Equipment	Brand/Model	Details	Target variable
SONAR	Garmin Fishfinder 250	single -frequency 200 kHz	Depth
GPS	Garmin GPS72s		Location
Measuring rod		2m in length	Depth

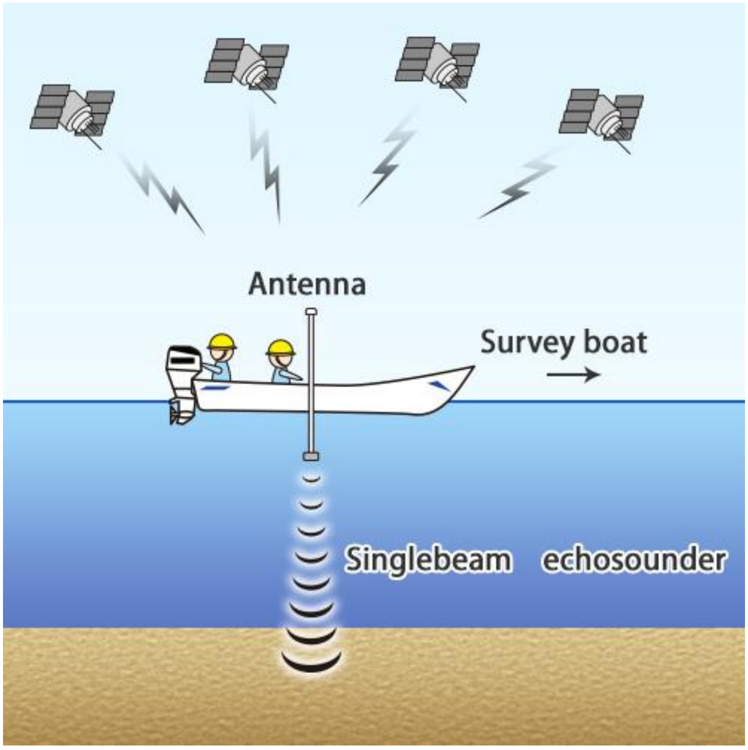

Figure 3.5: SONAR system set up (Ocean Engineering Corporation, 2015).

3.3.1 *Equipment*

The basic set up of the SONAR system is depicted in Figure 3.5. This set up, used in various studies connected to the ITC, has already proven successful (Leyton, 2008; Ndungu et al., 2013). The SONAR sends a 200kHz sound wave downwards, which is subsequently reflected by the river bed. The time between sending and receiving of this signal is then used to calculate the local depth. An important limitation for the SONAR is the minimum depth requirement of ca.

0.6m. This limits the SONAR usability in the more shallow areas which are present along the sides of the channel and further downstream. Another issue has to do with the stability of the boat. When the SONAR beam is not directed straight down, a biased (larger) depth will be observed. This can be due to a less than perfect set-up of the sounder, but also because of instability of the boat caused by paddling and/or waves.

All depth measurements are recorded together with their respective latitude, longitude and time by the Garmin GPS72s. Accuracy of the GPS72s is always shown by the device on its display and has been field tested and confirmed. When using it under field conditions accuracy in latitude and longitude was estimated at 5 m. Only in some cases, for instance in close proximity to sporadic larger vegetation, the accuracy was less.

The SONAR has been mounted on a canoe as depicted in Figure 3.6. Although it takes quite some effort to paddle the canoe up and down the river several times, its shallow draft proved to be a great attribute in these waters.

FIGURE 3.6: CANOE AND SONAR.

3.3.2 RIVER WIDTH

In order to capture the shape of the river images from Google Earth were downloaded. With Google Earth it is possible to use historical time series, and most relevant seemed to be the images from 20-12-2012. These images show a wide river in the downstream area, suggesting a situation of relative high water. Also they were taken in the same month as the field study was taking place, and are relatively recent, so the shape and width of the river is likely to be the same. These images were downloaded, georeferenced and imported into a GIS.

Of course the accuracy of the width could be easily tested in the field. The width of the river has been recorded at several locations along the river and was subsequently been compared with the widths found in the Google Earth images. This appeared to be accurate.

3.3.3 *Sampling method for depth data*

Concerning the method of surveying some suggestions can be found in literature (see Figure 3.7). In all examples information on transects is of major importance. This is often captured by taking manual cross sections or surveying in a certain navigational pattern. In the latter case the longitudinal variation is also captured in the pattern.

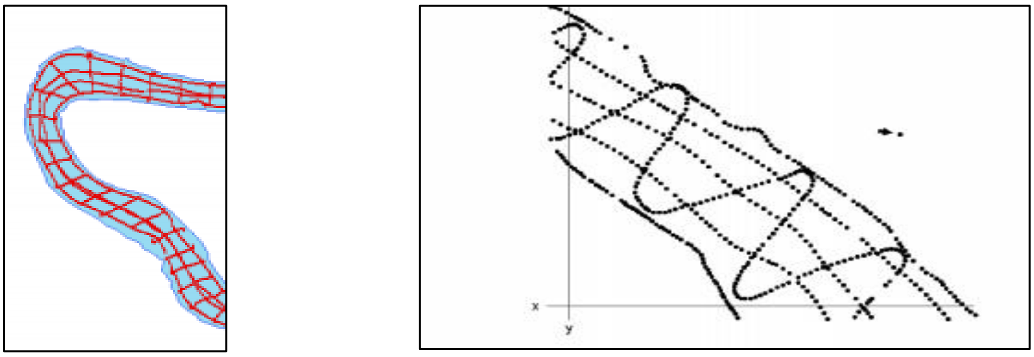

Figure 3.7: Bathymetrical survey patterns. Left example from (Vaughan et al., 2011) Right example from (Rogala, 1999).

In Heuningnes river however the situation is far from ideal. An optimum solution had to be found while acknowledging the constraints of time, equipment, low discharges and tidal variation. For this, the river was subdivided in four sections. Each of these sections having a different optimum approach for acquiring the bathymetrical data, because of their specific characteristics. This is illustrated in Figure 3.9.

Section 1

At the time of visiting section 1 is characterized by its shallow depths and limited width. Typical depth was between 0 and 0.5 meter, making it unsuitable for SONAR measurements. In this area manual measurements were the best approach. Cross sections have been measured by taking the depth relative to the water level for every meter from one side of the river to the other. This has been done by first setting up a tapeline across the river (see Figure 3.8) and marking its location on the GPS. Then the measuring rod was taken and depths were read for every meter across, with centimeter accuracy. Additionally it has been noted for every point whether reed was present or not. This information may prove useful in later stages when calibrating for roughness. In total 43 cross sections have been measured in section 1 which covers roughly 2.6 km. Decisions on where to take a cross section have been made in the field based on the observed variability in the shape of the river bathymetry. In the more variable areas more cross sections have been measured. These cross sections have in a later stage been longitudinally interpolated over the prepared grid to give the best representation of the real bathymetry.

FIGURE 3.8: TAPELINE FOR MANUAL MEASUREMENTS OF CROSS SECTIONS. (ABOVE LEFT) TAPELINE AND SILVER MEASURING ROD FOR READING DEPTHS, (ABOVE RIGHT) TAPELINE WHICH HAS BEEN FIXED IN POSITION, (BELOW) OVERVIEW OF MANUAL DEPTH MEASUREMENT SET UP.

Section 2

In section 2, depth increases considerably with depths mostly between 0.5 and 2 m. This made it possible for the SONAR to be utilized. Width however was still rather limited. Typically less than 7 m. With a canoe of 4.1 meters long this made navigation difficult when trying to acquire the depths for the transects. Moreover the accuracy of the GPS which is estimated at about 5 m, further problematizes an approach of navigating the transects. For this reason instead of sailing in a cross-sectional pattern, data has been acquired along three longitudinal lines. One in the center, and the other two at approximately 1.5 m from the river bank. Since we then also knew where all points should have been with respect to the river banks, all points were subject to locational correction afterwards. For the interpolation the bed level on the river sides was assumed based on my field experience and early model results, which will be discussed in later chapters. Using these data and the data gathered in the SONAR survey, first a number of transects were interpolated at points where data points were relatively abundant after which a longitudinal interpolation was done over the prepared grid.

Section 3

Section 3 was characterized by a wider and deeper channel. However in this more downstream section tidal influence was also significantly larger. While in section 2 tidal range was between 10 and 40 cm depending of the spring neap cycle, in section 3 this was measured to be between approximately 20 and 70 cm. It was thus important to use the high spring tides for the SONAR surveys in an effort to least limited by the SONAR's minimum depth requirement. A navigational pattern was chosen which gives information on the transects as well as the longitudinal changes in the bathymetry, while making sure this was to be completed within the available time of spring high tide. For the interpolation the same method as in section 2 has been applied.

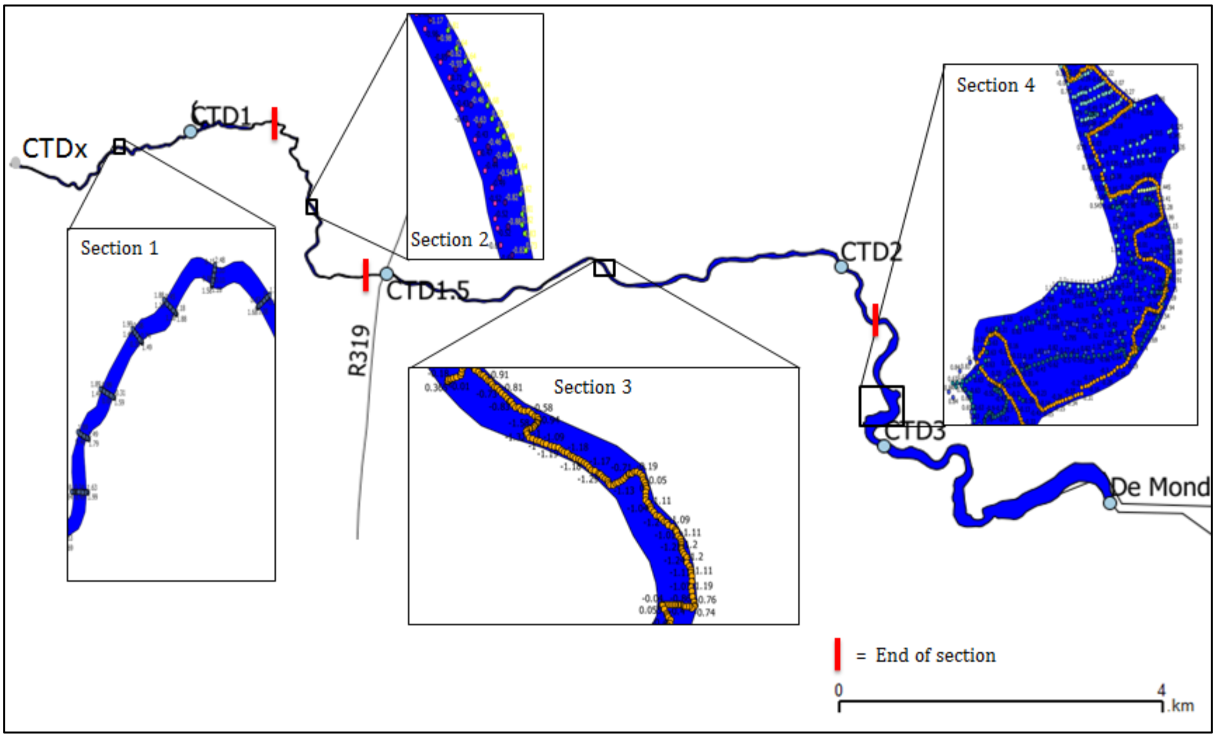

FIGURE 3.9: HEUNINGNES RIVER DIVIDED INTO FOUR SECTIONS, EACH WITH THEIR OWN OPTIMUM DEPTH SAMPLING METHOD.

Section 4

Section 4 was similar to section 3. Only in section 4 the river became estuarine. Some more wider, more shallow areas were present and the tidal range increased to its peak of 1 meter. In this section a combination has been made between SONAR and manual measurements. First a SONAR survey was completed after which data poor areas were identified and manually measured by means of the measuring rod, pen, paper and GPS. A pattern like in Figure 3.9 resulted. Also in this area the same interpolation method as in section 2 and 3 has been applied.

3.3.4 *SONAR HEAD OFFSET AND TIDE CORRECTION*

Before interpolation and after data collection all points needed to be corrected for two disturbances. Also the depth data needed to be referenced to a fixed level, so that all depth points, could be converted into bed levels. Firstly all SONAR data needed to be corrected for the SONAR head offset. As the SONAR head was mounted underneath the canoe, there was a certain offset which had to be added to the depth.

More complicated was the correction for the tide. As time passes, depth changes due to the tide. Also as the canoe moved along the river 'depth' changes, as tidal range changes while moving up- or downstream in the river. Both these factors were taken into account and with the help of continues water level observations at 6 locations along the river at the time of the bathymetrical survey: 'De Mond', CTDs 1, 1.5, 2, 3 and the temporarily installed 'CTDx' at the most upstream point of the river study area. All depth points have been collected with their corresponding latitude, longitude and time of recording. These points were then all corrected by using the linear interpolated referenced water level between two water level observation stations which monitored the water level at the time of surveying. This information could then be used to correct the surveyed depths. This was done in a semi-manual way correcting all points in groups where correction deviated less than 0.5 centimeter.

3.4 DISCHARGE

Heuningnes river at the time of visiting was still ungauged. This meant regular measurement of discharge had to be taken. In order to get an idea on how much water flows into Heuningnes river from Soetendaalsvlei, the discharge was measured at a location between Soetendaalsvlei and CTD1. Available equipment is listed in Table 3.2 below.

TABLE 3.2: EQUIPMENT FOR DISCHARGE MEASUREMENTS.

Equipment	Brand/Model	Details	Target variable
Flow meter	OTT C20	Range 0.035 - 5 m/s	Flow velocity
Tapeline			Width, Depth
Stopwatch/twig			Flow velocity

On location it became clear quite quickly that flow measurements in a wider section were not possible due to the low discharge in the river. This also ruled out any dilution gauging measurements because of the absence of turbulence. The solution found was to use a location where flow was heavily constricted, and regularly estimate the flow at that location.

One such location was found where the river was forced through a culvert under an old bridge (see Figure 3.10) located next to location CTDx. Seepage was blocked as much as possible by placing sand and rocks in front of all cracks that were visible (see Figure 3.10 right).

FIGURE 3.10: CONSTRICTIVE POINT USED FOR DISCHARGE MEASUREMENTS.

Measurements were taken using the OTT C20. Flow velocity was measured at the exit of the diver in the middle of the flowstream and at both sides. The average of these three flow speeds was taken as representative for the average cross-sectional flow velocity. Subsequently the width of the stream inside the diver was measured and assuming a perfect circle, the cross-sectional area was calculated. Multiplying both numbers gave an estimate for discharge through the diver.

In order to check whether this method was reliable the same procedure has been done at the entrance of the diver, as well as measuring flow velocity by simple floating test through the diver using a piece of reed and a stopwatch (the average of 5 float tests was used). All three methods gave similar results, confirming the accuracy of the methods.

Using the described method, the discharge was monitored for a period of 6 hours. To see if any tidal effect was measurable in the discharge. Generally only a gradual decline in discharge was measured over a period of several days, so only taking sporadic measurements was considered to be a valid approach. In practice this meant roughly once every two days when present in the field. With this declining discharge also the water level dropped. At a later stage only float measurements were possible due to the fact that the OTT C20 was not fully submerged anymore.

Between measurements linear interpolation has been applied. For extrapolation to dates before measurements started, a Q-h relation has been established using the available discharge measurements gathered, and the data from a depth gauge which was installed around October 2014 by the University of the Western Cape (UWC) at the measurement location. Allthough this was done with limited data, impact of discharge errors in the model is expected to be limited because of the small magnitude of the discharge.

3.5 DELFT3D

One of the most important tools for answering the posed research questions is a hydrodynamic model. In this thesis Delft3D (FLOW module) is chosen as the model to work with.

Delft3D has a number of advantages. First of all Delft3D is not only a hydrodynamic model, but is also capable of simulating several other processes including salinity. Secondly Delft3D is a model which can be set up for 1D, 2D or even 3D simulations. This ensures flexibility in case significant stratification is present and needs to be accounted for in the simulations. Thirdly, Delft3D is a model which has been applied by scholars for many years. Articles from the early 1990s can be found using Delft3D. It has thus been extensively tested and subsequently improved by newer versions of Delft3D. In this thesis, version 4.01 was used. Also at present, many studies successfully apply the model for salinity related issues with respectable results(Ge et al., 2011; Harcourt-Baldwin & Diedericks, 2006; Hu & Ding, 2009; Kurup et al., 1998; Lee et al., 2006; Nguyen, 2008; Van Breemen, 2008; van den Heuvel, 2010). But also on smaller scale rivers in the shallow estuaries or rivers of South Africa. Results of these studies indicate that Delft3D can be a very relevant tool in describing salinity in a shallow river (Van Ballegooyen et al., 2004). For Delft3D also significant in-house experience is present within University of Twente (UT), as well as in the University of the Western Cape (UWC). This enlarges the chances of success. Finally, Delft3D has been made an open source model since 2011. Although this is not an argument in terms of performance, it is valuable that open source models are being made most visible, so that its use gets promoted and it eventually becomes more easy for policymakers to support their decisions with proper scientific basis.

The core of Delft3D are the shallow water equations. These equations are derived from the three dimensional Navier-Stokes equations for incompressible free surface flow. The governing equations for salinity is the advection-diffusion equation. The model is spatially schematized in a grid which can be either 1, 2 or 3 dimensional. Grid cells do not have to be squared as Delft3D can work with the so called orthogonal curvilinear grid. Individual grid cells can deviate from one another as long as they obey to the minimum requirements for orthogonality, aspect ratio and neighboring cells size difference. Delft3D also allows for a distributed roughness.

3.6 SALT INTRUSION IN LITERATURE

In order to simulate salinity in rivers, many models have been developed. As a result of these models a number of scholars have found functions describing the salinity intrusion length into a river. Intrusion length is defined as the distance from the river mouth to the point where the background river salinity is reached again. Nguyen (2008) summarized some of the more important equations.

The first one was developed by Rigter in 1973. He based his equation on data extracted from the Delft Hydraulics Laboratory and of the Waterways Experiment Station and proposed:

$$L^{LWS} = 4.7 \frac{h_0}{f} F_D^{-1} N^{-1} \tag{3.1}$$

in which L^{LWS} is the intrusion length at the moment of low water slack, h_0 is the water depth at the mouth of the river, f is Darcy-Weisbach's roughness, F_D is the densimetric Froude number, and N is the so called Canter-Cremer number (Rigter, 1973).

The densimetric Froude number is defined as:

$$F_D = v^2 / \left(\frac{\Delta\rho}{\rho} g h_0 \right) \tag{3.2}$$

in which v is the tidal velocity amplitude, $\Delta\rho$ the density difference between sea water and freshwater and ρ the density of freshwater.

N expresses the mixing behavior in the river. The so called Canter-Cremers number, defined as

$$\mathrm{N} = \frac{\mathrm{W}}{P_t} = \frac{Q_m \tau}{P_t} \tag{3.4}$$

with W being the volume of river discharge Q_m over the tidal cycle τ and P_t being the tidal prism. For N<0.1 the vertical water column is expected to be well mixed, for 0.1<N<1.0 partially mixed and for N>1.0 development of a salt wedge is expected.

Similar to Rigter (1973), some more empirical formulas have been found. Fischer proposed a slight different formulation based on the same data (Fischer, 1974):

$$L^{LWS} = 17.7 \frac{h_0}{f^{0.625}} F_D^{-0.75} N^{-0.25} \quad (3.5)$$

And later Van Os and Abraham published (Van Os, A.G., and Abraham, 1990):

$$L^{LWS} = 4.4 \frac{h_0}{f} F_D^{-1} N^{-1} \quad (3.6)$$

Which is very close to the equations Rigter proposed in 1973. All these equations are based on a number of simplifications. They assume a single channel river of constant cross section and are based on steady state models.

Later more advanced formulations have been published by among others Savenije. In 1993 and 2005. These equations take the exponential shape of a river into account (Nguyen, 2008). However as the shape of Heuningnes river does not have a particular exponential (flute-like) shape, these equations will not be discussed.

In order to get a first estimation of intrusion length L, the empirical equations mentioned in paragraph 4.1 will be utilized. Input and results can be found in Table 3.3.

TABLE 3.3: INTRUSION LENGTH INPUT AND RESULTS.

Variable	Value	Unit	Reference
Estuary length	15000	m	Field estimate
Estuary width	35	m	Field estimate
Depth at mouth	0.5	m	Cape Nature, 2005
Tidal range	0.71	m	DWAF
Discharge Q	0.06	m3/s	Field estimate for 7-14 December 2015
Tidal flow amplitude	0.5	m/s	Estimate
f	0.126	-	Estimate
delta_rho	27	-	Average seawater density difference
rho	1000	kg/m3	Average freshwater density
t	44700	s	Tidal cycle
g	9.8	m/s2	
N	0.007195	-	
F_d	1.889645	-	
Rigter (1973)	1372	m	
Fischer (1974)	69	m	
Van Os & Abraham (1990)	1284	m	

As can be seen in Table 3.3, the equations give some questionable results. Especially the equation put forward by Fischer (1974) gives very low result, which is not plausible. Some of the input is rather difficult to define, for instance the depth at the mouth. In Heuningnes river this area is a very dynamic area, which makes it difficult to assign a static depth value. Also values contributing to the magnitude of the tidal prism are difficult to estimate without proper field measurements. This is also the case for the friction factor and tidal flow amplitude. Finally an average width has to be found, which can be subjective.

Although these values are somewhat arbitrary due to the uncertain input, it is interesting to see how they perform when compared to measured and modeled values, to be discussed in later sections of this report.

Also on possible stratification literature has suggestions. Stratification occurs when upstream water does not mix with the intruding sea water. Main reason for this is the density difference between sea water and fresh water. The water then forms two layers on top of each other, which is sustained by the absence of mixing forces. A very important mixing force is the tide itself. A larger tidal range giver a stronger mixing force. However this should be viewed relative to the channel depth, so i.e. combining a micro tidal environment with a deep channel (Haralambidou et al., 2010; Kurup et al., 1998). Another important force is that of the river discharge. When dealing with a low discharge, the tide will more easily mix the water over the vertical column. In the case of a high discharge stratification is more likely to occur, as a fresh water layer on top of the salty sea water is sustained by the constant forcing of the discharge. Similar theories are also found at different sources where is stated that the tidal prism needs to be larger than the discharge for the river to be vertically mixed (Savenije, 1986). This can also be evaluated using the earlier mentioned Canter-Cremers number. When its value is lower than 0.1, fully mixed conditions are expected (Nguyen, 2008).

It must however be emphasized that a single river can have different mixing types, in the spatial as well as temporal dimension. It can be for instance found that the lower reach is well mixed due to the tidal range, but the upper reach is stratified, since tidal range is damped further upstream. Also depending on discharge and spring-neap cycles mix type can change through time.

4. Measurement results

In this section all results from the field campaign will be discussed. First salinity and water level data is described, followed by the bathymetrical data and the upstream inflow observations. Then all issues encountered in the field will be discussed, and finally some preliminary conclusions based on the gathered data will be drawn.

4.1 Salinity and water levels

In Figure 3.9 locations of most data recorders are depicted. Only 'Uys bridge' is missing. This is a data logger installed by UWC, just upstream of Uys bridge which is just upstream of location CTDx (all within 10 meters of each other). All CTD locations have collected salinity as well as depth measurements on a 6 minute interval. The location 'Uys bridge' and 'De Mond' only observes depth, on a 30 and 12 minute interval respectively. The period over which depth and salinity data has been gathered can be found in Table 4.1.

Table 4.1: Data gathering during field work between November 2014 and January 2015.

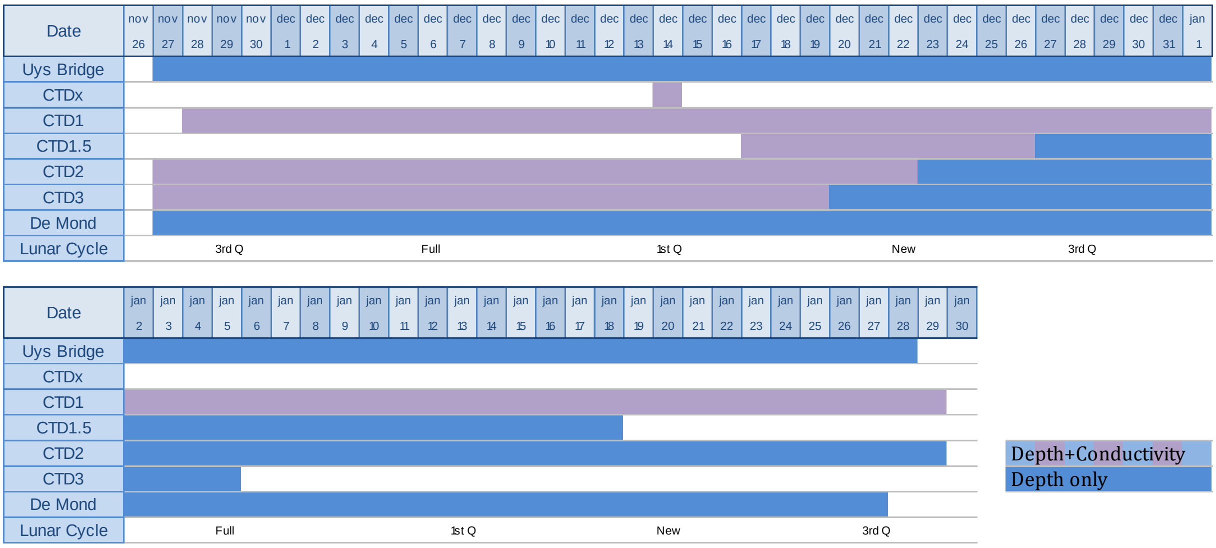

Periods of data collection show large differences. CTD1 has the most complete time series, no problems occurred here. Going further downstream towards CTD1.5 we find a much shorter time series. This has three reasons. Firstly, this CTD was installed some weeks later after analyzing the initial data. In addition an unknown person removed the CTD from its location 10 days before its scheduled removal. Thirdly, the salinity data seemed unreliable based on patterns observed in data from the other CTDs and was thus omitted. CTD2 produced very good depth data, but also this CTD showed problems in its later salinity measurements. This problem can be traced to organic development in the protective tubes in which the CTDs were installed. This organic development took about one month to close most of the perforation in the protective tube, not allowing for water to leave or enter the tube in which salinity was measured (see Figure 4.1). As this happened after about a month, it was only noticed when data was collected the second month. Similar problems were found for CTD3, also limiting the length of the time series for salinity. Unfortunately CTD3 also malfunctioned and no data could be downloaded after the 5th of January. Despite all these issues, this still leaves us with sufficient data to work with.

CTDx was a temporary station used for bathymetrical data correction which explains the short time series. The station at De Mond and Uys bridge are continuous stations operated by UWC and DWAS, respectively. The referred data period is a selection from the data available.

FIGURE 4.1: GROWTH OF ORGANISMS CLOSING CTD TUBES.

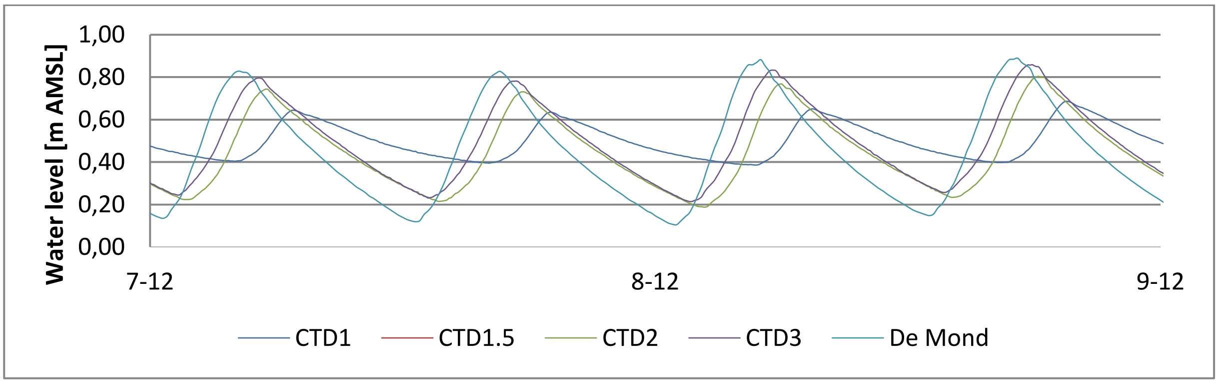

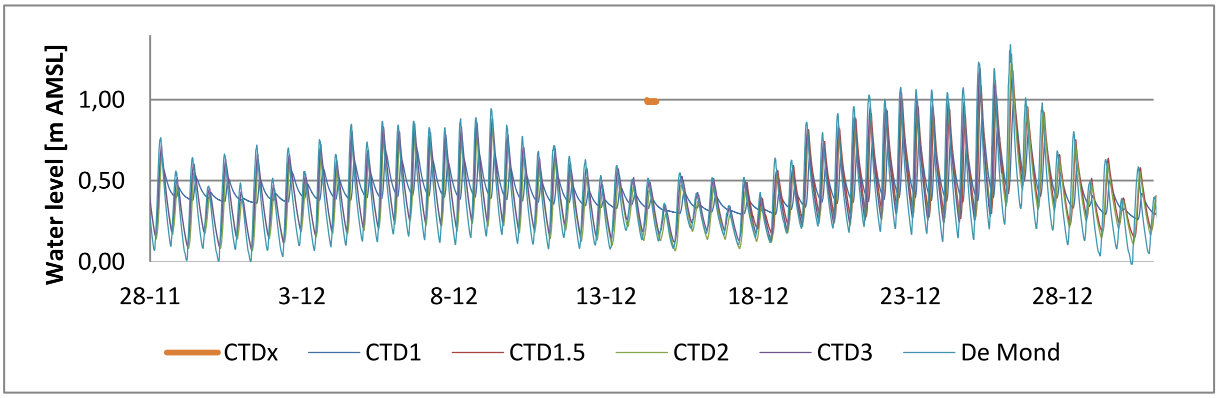

FIGURE 4.2: CORRECTED AND REFERENCED WATER LEVEL MEASUREMENTS.

Water depth data was referenced using a number of elevation points surveyed by the Ministry of Agriculture and was subsequently corrected for systematic errors. This systematic error was introduced when translating the measured elevation point next to the river, onto the exact location of the CTD in the water. The correction was done based on analyses of the first model results. Some results are shown in Figure 4.2. Concerning salinity no corrections were done. The data is depicted in Figure 4.3. The complete overview of data can be found in Appendix C.

In Figure 4.2 a number of trends are clearly visible. On the longer term we can identify a clear spring-neap cycle, caused by the dominant semi diurnal (M2) tide. In the top graph of Figure 4.2 the decreasing tidal range, from downstream to upstream, is clearly depicted. The peak lag time decreases when moving upstream. For instance at 29-11-2014 the maximum water level is observed at CTD1's location 120 minutes later than at De Mond.

Figure 4.3 shows the salinity measurements for the respective CTDs. Also in this case we can identify a spring neap cycle when looking at the longer term data. Secondly a decrease in amplitude of salinity is visible when moving upstream. At CTD1 the amplitude is almost negligible. Another interesting observation is that CTD1 shows a clear increasing trend, starting at 1.6 ppt in early December and ending up at 10.1 ppt in late January. At this point also tidal influence becomes noticeable, with an amplitude in the salinity levels of about 1 ppt.

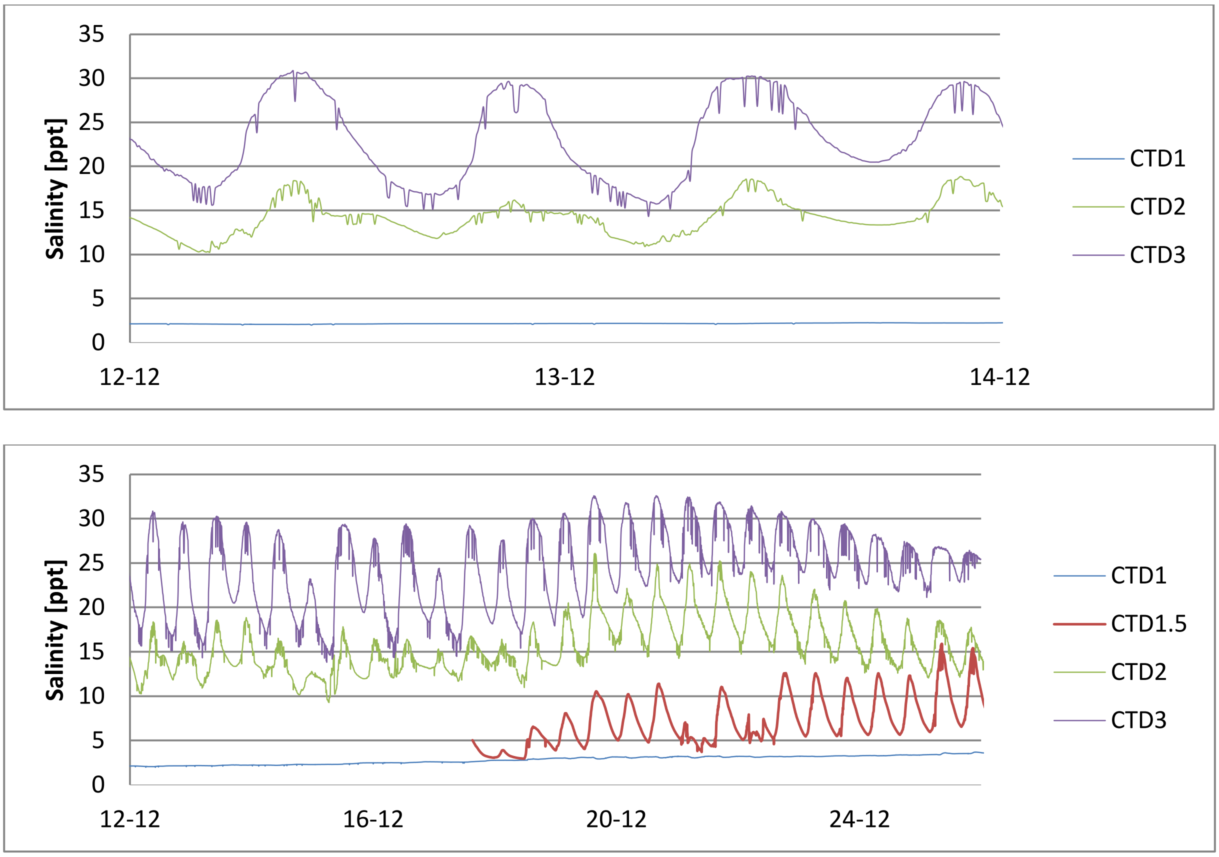

FIGURE 4.3: SALINITY MEASUREMENTS.

The overtime increase of salinity at CTD1 is likely due to a number of processes. As rainfall was almost zero, and summer temperatures and wind were significant, causing evaporation, this mounted up to a rise in salinity in Heuningnes river in general. Secondly this increase in salinity was not only in Heuningnes river, but also in its headwaters, causing the inflow to also increase in salinity. In addition diffusion of salt originating from the ocean may have added to the salinity in Heuningnes river, also affecting the upstream region, and finally subsurface flows from Kars river is a possible factor involved.

A number of data in Figure 4.3 are clearly lower than the data before and after. This can likely be attributed to measurement errors, since all other values follow a clear trend.

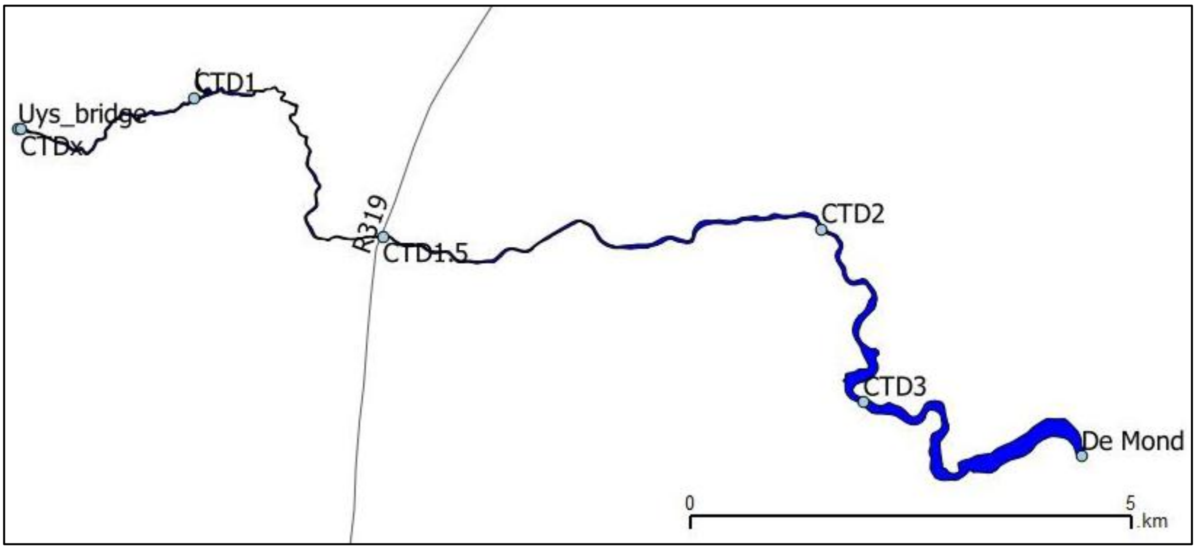

FIGURE 4.4: ALL LOCATIONS FOR WATER LEVEL OBSERVATION.

4.2 BATHYMETRY

A custom made grid for Delft3D has been produced using RGFGRID software, representing Heuningnes river which neatly fits over the river domain on Google Earth images from 20-12-2012. The channel is 5 cells wide and 1343 cells long. In order to have some kind of representation of the river banks, data on both the far left and right banks were overwritten by a river bank height of 1 meter AMSL upstream, and 0.3 meter AMSL downstream. The lower value for the downstream banks is based on the more flat characteristics of the area, and a river which cuts less 'clean' through the landscape.

The riparian areas which are most likely to be flooded with higher water levels are also covered by the grid. Three areas have been identified, all in the downstream area. The resulting grid can be found in Figure 4.5.

In the field a total of 8931 depth points have been collected. They have subsequently been corrected and interpolated as described in the methodology. The result can be seen in Figure 4.5.

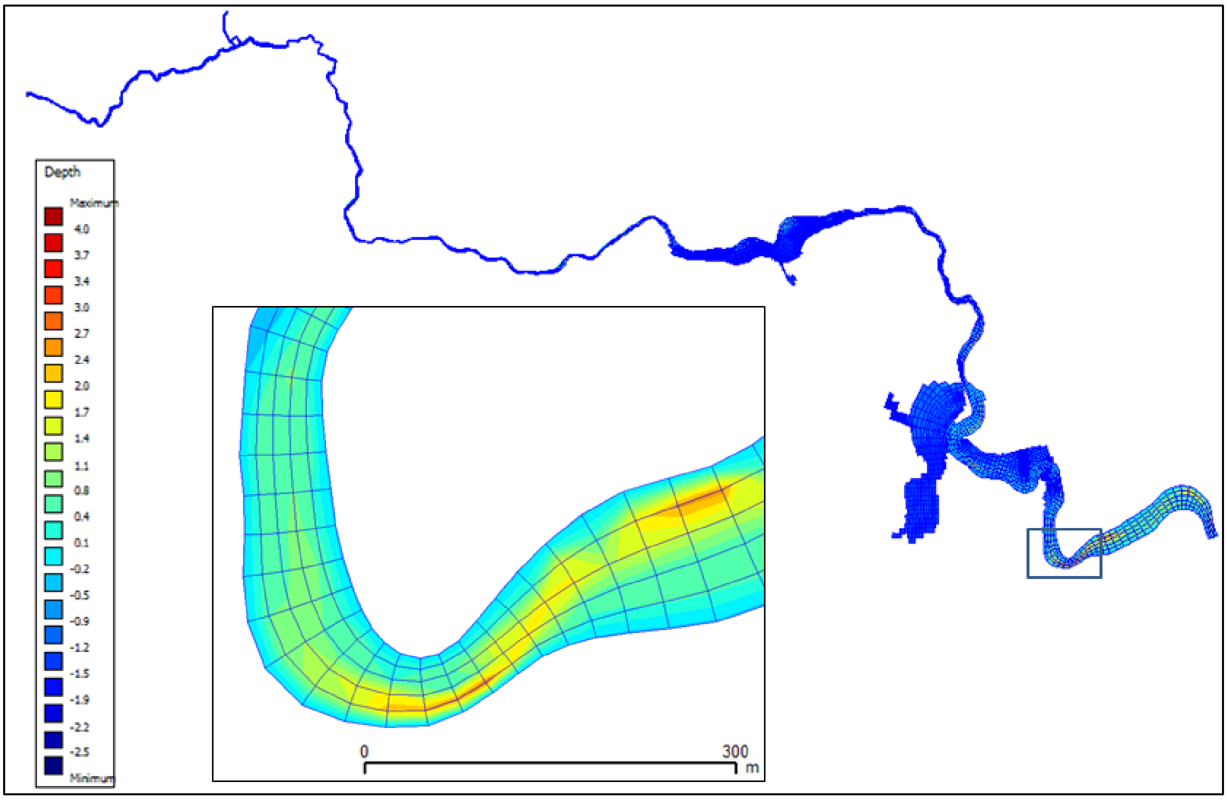

FIGURE 4.5: INTERPOLATED BATHYMETRY.

4.3 INFLOW AT THE UPSTREAM BOUNDARY

Discharge has been measured at location 'Uys Bridge' as depicted in Figure 4.4. The results are presented in Figure 4.6. The graph shows a clear recession curve, which is to be expected in the summer season. Discharge declined from 60 l/s to nearly zero.

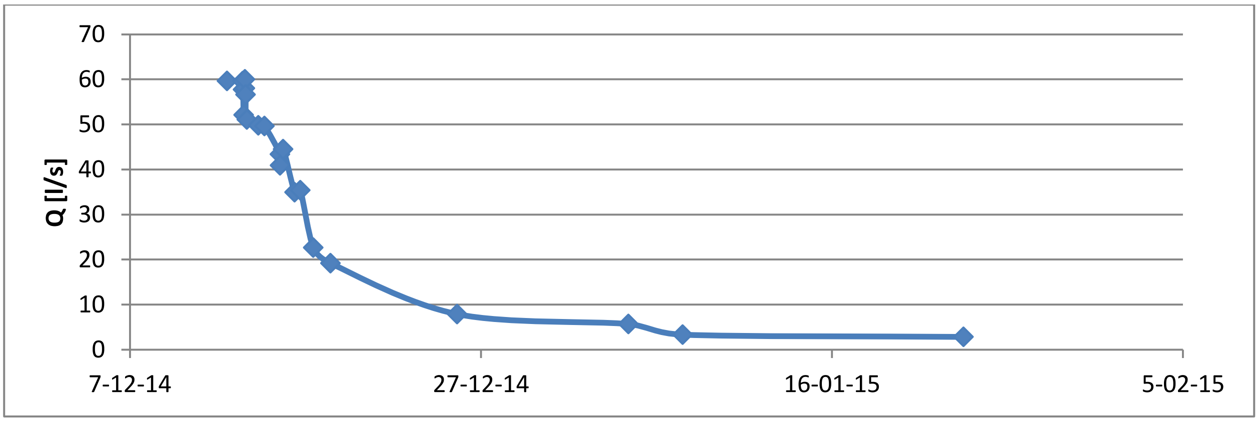

FIGURE 4.6: DISCHARGE OBSERVED AT UYS BRIDGE.

4.4 Discussion

Field data always comes with a certain degree of error. The data collected in and around Heuningnes river are no different. In this paragraph the expected error involved in all acquired data will be discussed.

Water level data

Water level measurements are coming from two separate sources. One source are the CTDs which were installed in the field. The second source is the data received from DWAS which gave water level measurements at the river mouth (De Mond). For the latter data source accuracy is unknown, as no information on accuracy was enclosed with the data. However as data is given in a format with three decimals, millimeter accuracy is suggested. Concerning measurements produced by the CTD divers, accuracy can be estimated. The manufacturer OTT promises a 2 millimeter accuracy with the used configuration (OTT, 2009). Errors due to changes in air pressure are eliminated as air pressure is monitored and corrected for by the CTD. Also the CTD is physically held into position in a robust way. Organic development in the tubes in which the CTDs were installed are not likely to have had influence on the depth measurements. Water was still able to exit the tubes when pulled out of the water, and also no evidence of decreasing amplitudes can be found in the data other than the spring/neap influence. Measurements are thus expected to be accurate.

Problems arose when referencing the data to a certain datum. The original plan was to measure the elevation of the water level at the CTD locations and record the timestamps at which this was done. These elevations could then be used to convert all depth data observed by the CTDs, into elevation data. If executed on a windless day (flat water) this would have given an error of approximately 1 centimeter coming from the small inaccuracy of the Trimble R6 GPS equipment used by the Department of Agriculture and the minimal fluctuations in the water level. Unfortunately due to bad GPS reception it was not possible to measure the elevation of the water level, and it was only possible to take measurements at higher ground. These measurements were subsequently used to acquire the elevation of the water level using a leveling instrument (see Figure 4.7). The leveling instrument is only accurate to about 5 cm and also wave action added an additional uncertainty as waves make it difficult to determine the exact water level. This introduced a systematic error into the water level data.

Figure 4.7: leveling instrument set up.

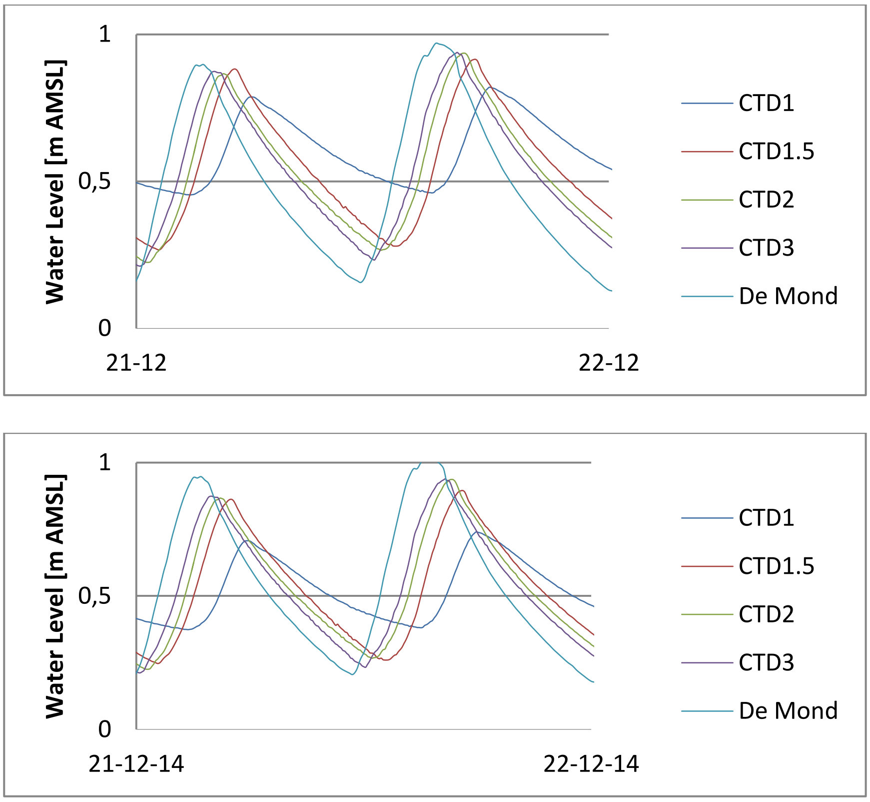

FIGURE 4.8: (TOP)WATER LEVEL DATA UNCORRECTED, (BOTTOM) WATER LEVEL DATA CORRECTED .

In the case of CTD1.5 and CTD3 another problem was encountered. Both CTD divers were either removed or malfunctioning at the time of taking referencing measurements. To solve this issue the height difference between the referenced point next to the river, and the actual level at which depth measurement were taken had to be determined. This had to be measured by hand while standing in the middle of the river, again introducing additional uncertainty. The error which comes from this uncertainty is estimated to be between 0 and 15 cm. This was corrected based on first analyses of model simulations, resulting in a correction of -0.09 m for CTD1, -0.02 m for CTD3 and +0.06 m for De Mond, as shown in Figure 4.8.

SALINITY DATA

All salinity data originates from the CTD divers placed in the field. The first period, all this data is considered accurate. However, as already discussed briefly in section 3.2, problems arose on the longer run because of organic growth on the protective tubes of the CTD divers. It is clear the last period of data cannot be trusted, however somewhere in between the first and last period it becomes difficult to assess whether data is trustworthy. The decision on which data not to use has been made based upon visual inspection. Patterns from salinity levels should more or less follow a similar trend as the water level. Based upon this knowledge, only the first month of data of CTD2 and CTD3 are considered trustworthy.

CTD1.5 was installed three weeks later and shows incoherent data. Subsequent tidal cycles of salinity data are very variable, which is not to be expected when all other stations show a very stable trend. An explanation may be the location where the CTD was installed which was just upstream of some vegetation in the middle of the river. Perhaps this somehow interfered with the salinity measurements.

Bathymetrical data

When testing the GPS for its accuracy in terms of latitude and longitude it was established that under most circumstances it could be accurate up to 5m. This was tested by laying a 100 m tapeline along a soccer field sideline, and taking a reading every meter. Upon inspecting the result a maximum inaccuracy of 5 meters was found. In river section 2 (as divined in Figure 3.9) correction for this error could easily be done, as the path of surveying was known and identifiable in a GIS. For all other sections in the river this error has been corrected where possible, however it was not always possible to know where exactly was surveyed as field circumstances regularly forced for minor changes to the navigational pattern.

Although the SONAR itself may have a high accuracy, field conditions have their influence. The SONAR has been mounted underneath a canoe. Possible problems come from the SONAR measuring in an imperfect angle, and thus overestimating depth. While the canoe was rather stable and most of the surveying has been done on calm water, there is still uncertainty being introduced in this way. Another source of uncertainty is the influence of salinity on the SONAR, as the pulses travel at faster speed through salty than through fresh water (Coppens, 1981).

Aside from errors in the depth measurements, the correction also brings uncertainty into the data. Between the six points at which the water level was monitored, the water level was linearly interpolated. This means no back water effects are accounted for, although they are most certainly present in a tidal area. Impact will however be limited since points are relatively close to each other (see Figure 3.3).

When surveying bathymetry more points are usually better. However the river bed level does not show very variable pattern, and thus limited measurements should eventually yield a good estimate of the river bathymetry. Most problematic are the shallow areas. The most important shallow areas have been measured manually after inspection of the SONAR results. However not all locations where SONAR points were relatively scattered, have been covered by supplementary manual measurements. This again, was due to time constraints.

In order to fill in the blind spots in the bathymetry, an assumption on the river banks was made. Although river banks are variable in height, on most places they were just 30 to 100 cm above the water level depending on the tide. For the upstream section 100 cm has been used for the banks, while in the downstream more flat region 30 cm was deemed more suitable. This definitely introduces an error into the bathymetrical data set, but it is the best approach with the means at hand.

Aside from these shallow areas, also two ‘overflow areas’ are identified. In these areas the elevation of representative points are measured by means of a leveling instrument. Notes have been made on the shape and size of the area which is represented by that point and the area is subsequently entered in a GIS. This comes with a clear level of uncertainty as the areas look different on a satellite picture as it does in real life, and thus errors are bound to be made when extrapolating the representative points.

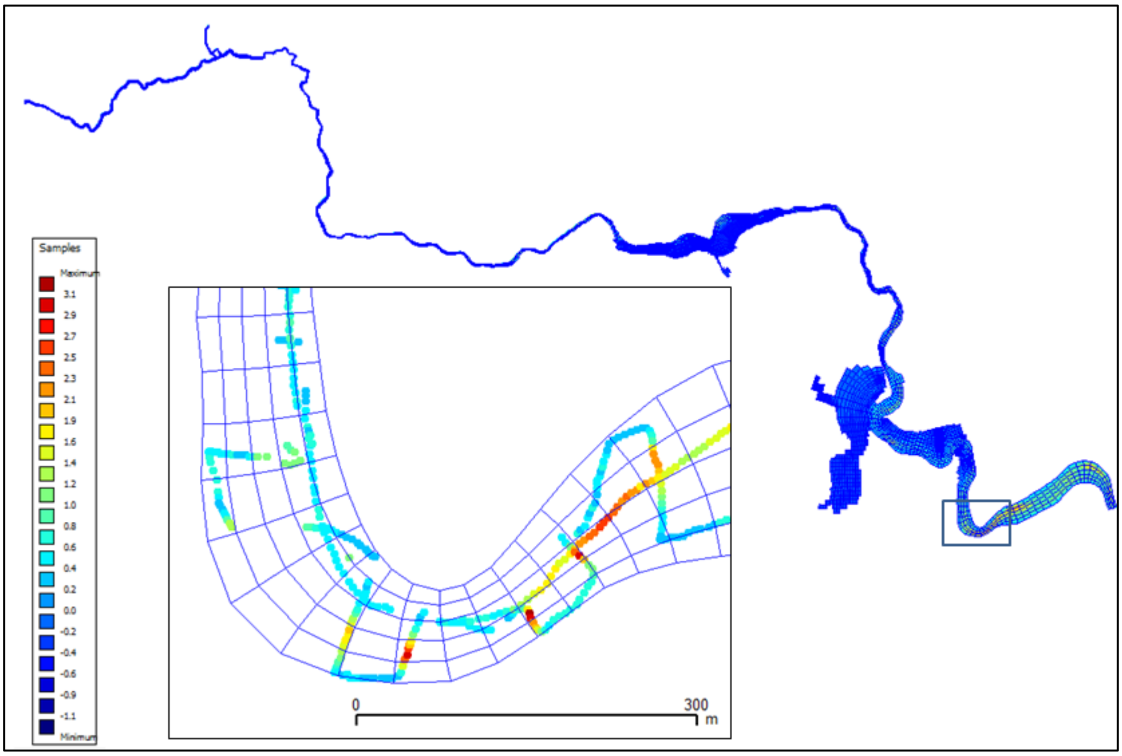

FIGURE 4.9: GRID AND MEASURED DEPTHS.

When extrapolating the point measurements to the bathymetrical grid, more uncertainty is introduced to the data set. In Delft3D, all grid cell intersections are the nodes at which depth is calculated. Ideally there are multiple measured points around one such node, so that an average can be used as the interpolated bathymetrical elevation. In most instances however, this is not the case. To fill the gaps in the bathymetrical data set an interpolation method was applied, which always causes additional uncertainty. However with the primarily longitudinal interpolation applied, and the fact that the river bed showed only limited spatial variability at the time of visiting, accuracy of the interpolated bathymetry is believed to be accurate enough for modeling purposes.

Variability of the bathymetry over time is not investigated. In personal communication with local residents siltation was mentioned to be rather large, and also bend erosion was taking place. This latter process even creating the necessity for placement of a submerged wall to protect the outer bend. This shows that there definitely is a variation in the time domain, however not on the shorter term (three months) in which the field study was executed.

DISCHARGE DATA

The method used to measure the discharge has a number of deficiencies. To start with, only the discharge through the culvert has been measured. Any additional discharge flowing through the cracks of the bridge, is not taken into account. Also there might be water going into the culvert, but then falling through a crack in the diver and exiting the bridge through another crack. However when inspecting the bridge only one location was found where seepage through the bridge was noticeable. This place has subsequently been carefully blocked by soil and rocks, blocking most but not all of the flow. This might have caused a slight underestimation of the discharge.

After 15-12-2014 the water level in the culvert was too low to sustain measurements being taken anywhere but in the center of the channel and in the center of the water column. This on its turn may have caused a slight overestimation of the flow speed, as flow speeds are likely to be smaller closer to the sides and closer to the bottom due to friction.

Another interesting discovery was done on the final day of fieldwork. The water level at CTD1 was 50 to 60 cm lower than the water level at Uys Bridge (depending on the tide), while the distance was only 2 to 3 km apart. This water surface slope seemed much too high, as almost no flow was noticeable this far upstream in the river. This leaves either the possibility of a very large roughness, or perhaps more likely, the possibility that both parts of the river are not (well) connected anymore.

4.5 PRELIMINARY CONCLUSIONS

By gathering these data a good insight into the Heuningnes water system was obtained. A decreasing tidal range was measured along the channel, a tidal range of 0.74 m was dampened to 0.33 m when reaching location CTD1 at 16 km upstream from the river mouth. The tidal lag between these locations was observed to be 3 hours and 36 minutes. Flow speeds were generally very low in Heuningnes river. Only in severely constricted areas such as at Uys Bridge (see Figure 4.4 and Figure 3.10) a river flow was measurable. In addition of course flow caused by incoming and outgoing tide was measurable in the more downstream area. The discharge observed entering the river upstream was of 0.06 m^3/s at the start of December 2014, declining to about 0.003 m^3/s in January 2015.

Stratification of salinity was not expected in Heuningnes river, as literature suggests a fully mixed river when a shallow river or low discharge is combined with a relatively large tidal range (see section 3.6) . This proved to be true when taking measurements along the river between CTD1.5 and De Mond. As the Canter-Cremers number was already calculated to be much smaller than the threshold value of 0.1 for mixed conditions, further investigation of possible stratification under different tidal circumstances and at different moments during the tidal cycle were not deemed necessary.

Sources for salinity in Heuningnes river have readily been identified. Of the three possible sources mentioned in section 2.6, one can be ruled out: runoff from within Heuningnes catchment. As there was virtually no rain in the catchment between the end of November 2014 and the end of January 2015, all salinity observed in that period must have come from either the Indian ocean, or the upstream inflow. Upstream inflow was first observed to be 1 ppt, increasing to about 4 ppt in late January. This alone does not account for the increase in salinity observed at CTD1, increasing from 1.6 ppt to 9.8 ppt between the start of December and the end of January. On the longer term, additional factors like diffusion and evaporation apparently play a significant role.

Largest influence on salinity deducted from the observed data is the downstream water level, i.e. the tide. Figure 4.3 shows the salinity at CTD1, CTD2 and CTD3 as a function of time. For CTD2 and CTD3 a clear tidal influence can be seen. Also when analyzing the longer term salinity we can identify a spring-neap cycle in the salinity values of CTD2 and CTD3. In addition this data shows that the salt intrusion is at least as far as CTD2, which lies 7.8 km upstream of the river mouth. At the moment of low water slack we are still dealing with elevated salinity levels.

When comparing this to the equations found in literature it is clear that these equations largely underestimate the salt intrusion, as Rigter's (1973) equation suggests a salt intrusion at low water slack of 1.4 km. It does not seem likely that the gap between the observed 7.8 km can be closed with more accurate input, or at the very least shows that these equations are not capable of giving a quick realistic idea of the salt intrusion in this river.

The discharge is the second important forcing determining the salt intrusion. However its influence is up until now difficult to define as only limited variability has been measured in the discharge. Also comparing the data from the second month with the data from the first month is not possible due to data contamination of the second month, as mentioned in 4.1. Influence of the discharge is better analyzed with model results, to be discussed in the next section, were also answers concerning the influence of RSLR will be given.

5. MODELING

In this section the modeling part of the thesis will be discussed. First the objective of the modeling will be formulated, followed by a description of the model input and calibration details. In 5.4 the results of the calibration will be presented and explained, as well as the results for the scenarios. In the final section a discussion on the modeling part will be described.

5.1 OBJECTIVE

Firstly, the model needs to be calibrated, such that the observed water levels and salinity levels are reproduced using the observed boundary conditions. The parameters to calibrate are the roughness, eddy viscosity, eddy diffusivity, and at crucial locations the bathymetry.

This will result in an representative parameter set, which can subsequently be used to simulate RSLR and the effect on the salinity distribution in the model domain. These results will form an answer to the second research question as posed in Chapter 1 of this thesis.

5.2 MODEL SCENARIOS

The model is being run in 2D(h) since no vertical stratification has been found throughout Heuningnes river at the time of data collection. The scenarios which are to be executed can be found in Table 5.1. There are two sets of scenarios. First set 'A', consisting of three scenarios. These scenarios are to show the current situation compared to what it would look like when RSLR instantly imposed on the observed situation. First scenario is the calibrated scenario which forms a baseline to compare the second and third scenario to. Then for the second scenario a 0.52 m RSLR is imposed on the downstream BC. Finally in the third scenario the RSLR is combined an upstream BC set to 0 m^3/s. The chosen RSLR is roughly in the middle of the RSLR suggested by the various models described in AR5 of the IPCC, 0.4 m to 0.7 m (see section 2.7).

The second set of scenarios, set 'B', is one where a looped BC has been applied. This means that one observed cycle has been selected, which is then looped infinitely. This way it is easier to observe if and when the model has reached its dynamic equilibrium, defined as a state in which the difference in salinity levels between two consecutive tidal cycles is less than 0.25 ppt. In addition, it is easier to isolate the effects on the salinity by the changed parameters and or changed BCs. Set B also encompasses three scenarios. First a scenario without RSLR is simulated, which forms the baseline for the other two scenarios. Then a scenario with 0.52 m RSLR is executed, followed by a scenario using the highest water level peak observed between 2010 and 2015. In set B discharge is set to zero, so that all effects can be attributed to the change in the downstream BC.

TABLE 5.1: MODEL SCENARIOS.

Set/ Nr.	Name	Upstream BC (discharge)	Downstream BC (water level)	Short description
A1	Calibrated	Q observed	WL obs.	should give obs. water and salinity levels
A2	+0.52	Q observed	WL + 0.52 m	RSLR 0.52 meter
A3	+0.52Q0	Q=0	WL + 0.52 m	RSLR 0.52 meter, summer
B1	No RSLR	Q=0	WL obs. loop	Observed scenario, looped
B2	Loop +0.52	Q=0	WL + 0.52 m	RSLR 0.52 meter, summer. looped
B3	Loop +0.52max	Q=0	WLmax + 0.52 m	RSLR 0.52 meter, summer, highest water level peak between 2010-2015, looped

5.3 INPUT DATA AND CALIBRATION

This section will systematically describe all input data and calibration details of these input data. Wind force, although present in the study area, is being neglected.

The simulation period used starts 07-12-2014 at 05:24. This is during a time of spring tides. The simulation period extends over a little more than one week until 14-12-2014 at 18:36 when tidal range decreased at the downstream BC due to neap tides.

5.3.1 UPSTREAM BC: DISCHARGE AND SALINITY

Concerning discharge, the observed values (see Figure 4.6) have been assumed correct and have been loaded into a Delft3D boundary condition file. Values between observations have been linearly interpolated. Salinity observations have also been linearly interpolated.

5.3.2 DOWNSTREAM BC: WATER LEVELS AND SALINITY

For the downstream boundary condition the data observed by DWAS at the mouth of the Heuningnes river have been used (see appendix C). Observations are taken using a 12 minute interval, and linear interpolated is applied to acquire a smooth data set through time. As described in Chapter 4 some uncertainty was introduced when referencing all the water level data to a common datum. Based on model results, the water level observations were corrected by +0.06 meter. Salinity is kept constant at 33.8 ppt based on a water sample taken at De Mond.

5.3.3 BATHYMETRY

The bed level data have been projected on a curvilinear Delft3D grid which consists of 5 cells over the width of the river. Initial runs showed better results with a higher grid resolution, however due the large increase in model run-time the lower 5 cell resolution has been used. This gives some problems in the more downstream area of the model domain. Here the bathymetry is less constant, and more wide and shallow, making it harder to capture all the variability in this (low resolution) grid. Early results showed that too little water was able to flow through the downstream area of the model. Analyses of depth averaged flow velocities in this area showed a number of places where flow was obstructed due to interpolation over the (probably too coarse) grid. In these areas the bed level was lowered, so that enough water could pass through the area. An overview of the before and after situation can be found in Appendix B.

5.3.4 *INITIAL CONDITIONS*

Initial conditions for the model are threefold. The initial water level needs to be known, an initial value for salinity, and an initial value for flow speed in both x and y direction. All these values are distributed, meaning they have to be known for each grid cell.

In order to overcome difficulties in getting the flow velocities right, a carefully chosen starting time for the model scenarios was selected: the moment of high water slack at CTD2. Also considering the influence of the growth of organisms in the tubes (see Figure 4.1), an early starting date would be best, so December 7th 2014 at 05:24 was selected. The moment of high water slack at CTD2 means not only that flow velocities are close to zero for the most important areas of the model, but also water levels are more or less equal. The values observed at the CTDs have been implemented and subsequently interpolated. Values between CTDs have also been calibrated based on early model results.

For scenarios with a looped BC, water uniform water levels have been assumed, equal to the level of the BC at the start of the simulation.

The initial conditions for the scenarios with RSLR contain elevated water levels, however the same salinity levels are used as were used in the scenario without RSLR. As a result of this the model will need some time to find a dynamic equilibrium in most scenarios.

5.3.5 *ROUGHNESS*

Initial runs with uniform calibration showed unsatisfactory results. Most importantly differences between observed and simulated water levels upstream were too large. From field observations it can also be reported that more reeds and obstructive vegetation is growing in the upstream section of Heuningnes river. A different roughness between upstream and downstream areas thus seemed a fitting solution. This resulted in a Chézy roughness coefficient (see equation 5.1) of 16 $m^{1/2}/s$ for the upstream section and 40 $m^{1/2}/s$ for the downstream section. In between, a transition area with Chézy roughness coefficient 25 $m^{1/2}/s$ was implemented in order to smoothen the model and prevent unrealistic water level changes along the channel. Exact extent of these roughness areas are based on observations from the field and early analyses of model results, but cause a degree of uncertainty. In Figure 5.1 an overview can be found of the defined roughness.

$$C = 18 \log \frac{12H}{k_s} \qquad (5.1)$$

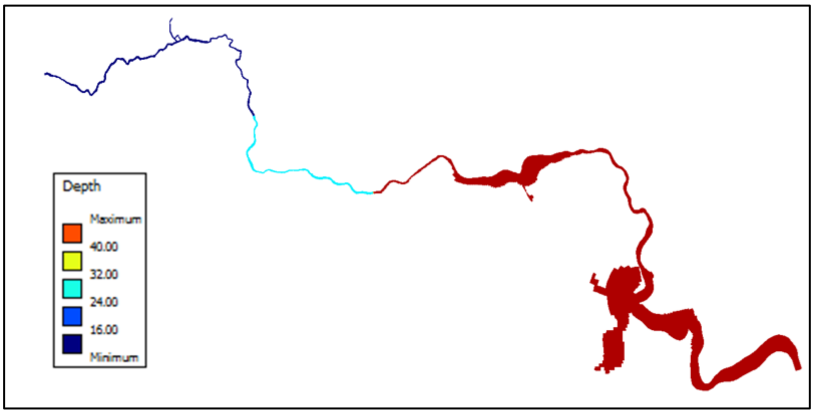

FIGURE 5.1: CHÉZY ROUGHNESS COEFFICIENTS.

5.3.6 *OTHER INPUT PARAMETERS*

Other important input parameters are the horizontal eddy viscosity, related to turbulent momentum energy transfer in the eddies, and horizontal eddy diffusivity, related to turbulent mass transfer and exchange by eddies. Eddy viscosity was estimated to be 1 m^2/s, whereas eddy diffusivity was set to 0 m^2/s, based on calibration results. Temperature is set on a uniform value of 23 degrees Celsius, density is assumed constant at 1000 kg/m^3 and gravity at 9.8 m/s^2. The time-step used for all simulations is 0.05 minute creating a runtime of 12 hours for a 1 week simulation.

5.4 RESULTS

In this section model results will be discussed. The first section will describe the calibration result followed by results from the scenarios proposed in Table 5.1. Finally the outcome of a sensitivity analysis is presented.

Results are shown for locations CTD1, CTD2 and or CTD3, see Figure 3.3. These results are evaluated using the graphical representation of the water level and salinity on these locations, as well as computing the R^2 and RMSE of the calibration simulations. Definitions of R^2 and RMSE can be found below.

$$R^2 = \left(\frac{\sum_{i=1}^{n}(O_i - \bar{O})(S_i - \bar{S})}{\sqrt{\sum_{i=1}^{n}(O_i - \bar{O})^2}\sqrt{\sum_{i=1}^{n}(S_i - \bar{S})^2}} \right)^2 \tag{5.2}$$

$$RMSE = \left(\frac{\sum_{i=1}^{n}(O_i - S_i)^2}{n} \right)^{0.5} \tag{5.3}$$

In equation 5.2 and 5.3 *o* represents observed values, while *s* represents simulated values. The number of values used in the equations is defined with *n*.

5.4.1 *Calibration results*

Calibration was executed in two phases. First hydrodynamically (phase 1), by optimizing bathymetry, viscosity and roughness. In the ideal situation only the roughness would have to be calibrated, however initial runs showed considerable lack of flow in the downstream area as discussed in 5.3. This was not readily solvable by calibrating with a roughness value only. So also bathymetry (as discussed in 5.3.3) and viscosity parameters were exploited to gain proper results. When a good fit was acquired, the fit for salinity (phase 2) was further optimized by varying the eddy diffusivity.

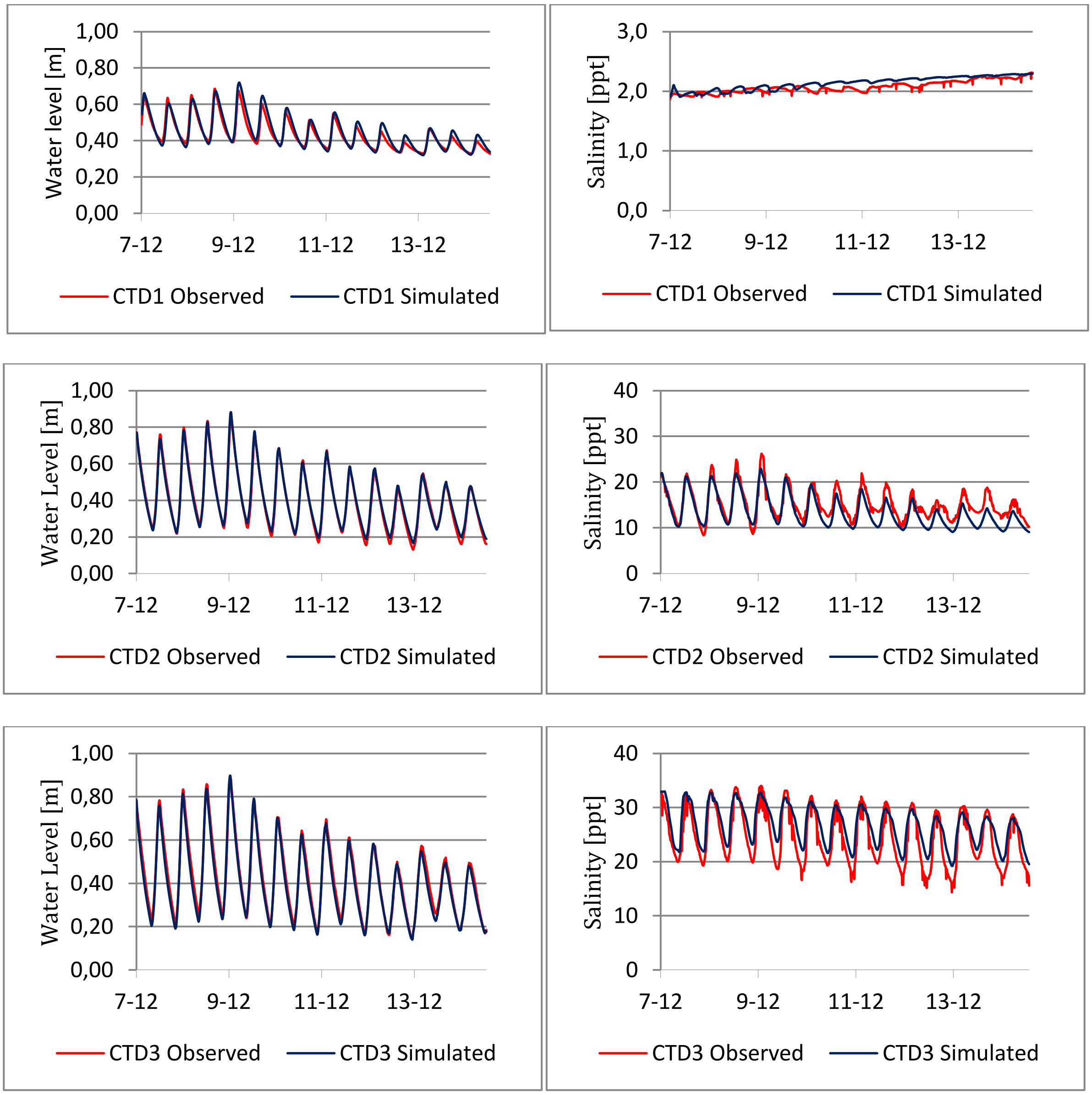

Figure 5.2: Calibration results of water levels (left) and salinity (right).

As can be observed in Figure 5.2, and from the model performance indicators in Table 5.2 the model performs well. Hydrodynamic results are close to observed values, with a R^2 value of 0.89 or higher and a root mean squared error (RMSE) of 0.02 or 0.03 meter. Salinity performs somewhat worse, showing a smaller amplitude which could not be calibrated further using the horizontal eddy diffusivity parameter, as this was already set to the lowest possible value of 0 m^2/s. The fact that the R^2 value of CTD1 seems to perform worse is partially explained by the fact that variance in this more upstream region is smaller. This is supported by the low RMSE for CTD1, for water levels as well as salinity.

When looking closer at Figure 5.2 it can be noticed that some tidal cycles show a small underestimation of the water level, while other cycles show a slight overestimation. These errors are however small and likely due to influence of wind on the river. When comparing wind direction and wind speed from weather forecasts (see appendix D) with the over and underestimations of the water level, it shows that overestimations are linked with easterly winds, and underestimations linked to westerly winds. This confirms the hypothesis, as the river roughly flows from west to east.

Salinity shows a somewhat larger error. CTD2 starts accurate but after a few tidal cycles shows an underestimation while CTD3 shows an overestimation of salinity. Apparently there is a lack of salt transport which cannot be explained by a lack of water transport, as water levels do not show such clear deviations. The inaccuracy is attributed to a number of uncertainty factors which are laid out in more detail in the discussion section. However size of the error is not uncommon for modeling studies like these. A modeling study done in the Selangor Estuary in Malaysia managed to stay within three ppt of the measured salinity values (Van Breemen, 2008).

TABLE 5.2: MODEL PERFORMANCE INDICATORS.

		CTD1	CTD2	CTD3	unit
Water level	R^2	0.89	0.93	0.93	[-]
	RMSE	0.03	0.02	0.03	[m]
Salinity	R^2	0.67	0.84	0.89	[-]
	RMSE	0.09	2.09	2.80	[ppt]

5.4.2 *FUTURE SITUATION*

Simulation of the future situation is done by executing scenario set A and B as described in 5.2 (also see Table 5.1). All results are shown for location CTD2. This location is far enough away from both model boundaries so that these do not bias the results, while also showing large variability in salinity levels, and thus possible changes to this variability. All results for salt profile migration are based upon CTD2 as well. First, the salinity profile is saved at the moment of maximum salinity level for CTD2 in the calibrated scenario. This same level (in ppt) is then found at a new location in the to be compared scenario. The distance between CTD2 and this new location is considered to be the salt profile migration.

Set A

Figure 5.3 shows the salinity results for three simulations. The blue line is the calibrated scenario as described in section 5.4.1. The green line represents the same scenario with only the downstream boundary condition elevated by 0.52 meter. The black line follows with 0.52 m RSLR and discharge set to zero.

In the first tidal cycles salinity was still adjusting to its new dynamic equilibrium, as all simulation started with the same ICs for salinity. Later in the simulation the different scenarios deviate more from each other as they find their ways toward their respective dynamic equilibriums. Whether these are reached is impossible to conclude. The spring-neap cycle in the downstream BC does not allow for a stable pattern as tidal range keeps changing. Differences may thus be underestimated in Figure 5.3.

In the final two tidal cycles we find an average increase of 1.1 ppt and a maximum increase of 3.6 ppt for the +0.52 scenario. The summer scenario with zero discharge shows an average increase of 3.1 ppt and a maximum increase of 6.2 ppt. Assessing the movement of the entire salt profile shows that it has moved 298 meter further upstream as a result of RSLR, and 579 meter in case RSLR in combined with zero discharge.

Aside from the increase in salinity we can also see an earlier peak of 48 minutes and an earlier trough of 60 minutes in the salinity graph. This can be explained by the higher water levels, and thus decreasing impact of the roughness.

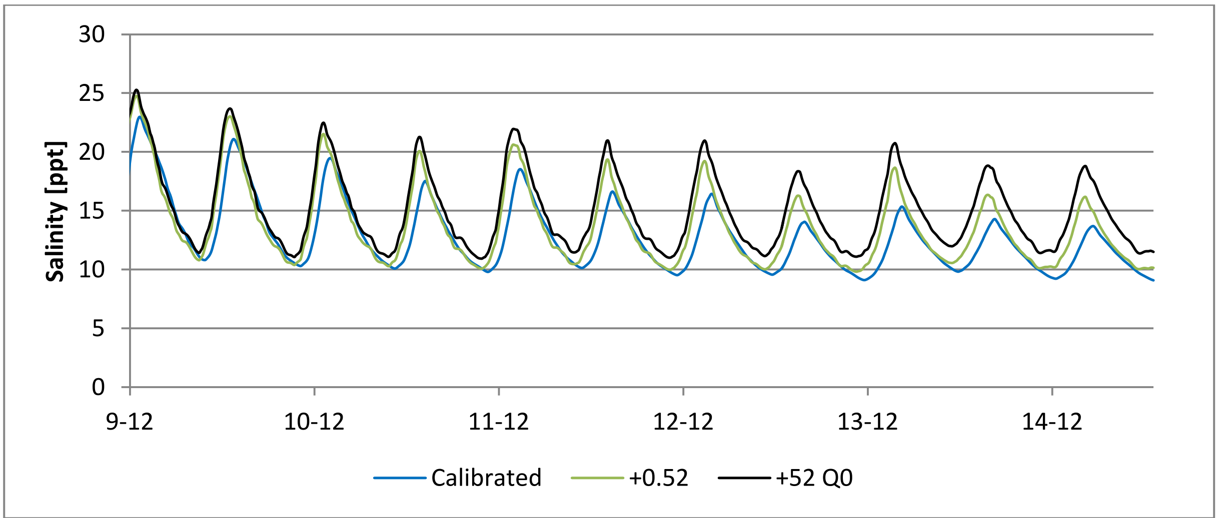

FIGURE 5.3: SALINITY LEVELS AT CTD2 FOR SCENARIOS +0.52 AND +0.52Q0.

Set B

Results for three different simulations are depicted in Figure 5.4. First concerning the scenario with only RSLR, we find that it takes the model 10 simulated hours, to find its dynamic equilibrium. The results again show a clear increase in salinity with an average difference of 0.35 ppt and a salinity peak level increase of 2.2 ppt. The movement of the salt profile is 397 meter in upstream direction which is in the same order as to what was found in the scenarios without a looped BC (see Figure 5.5). The graph also shows an earlier peak, with a difference of 36 minutes, which can also be attributed to a declining influence of the roughness over the larger water column.

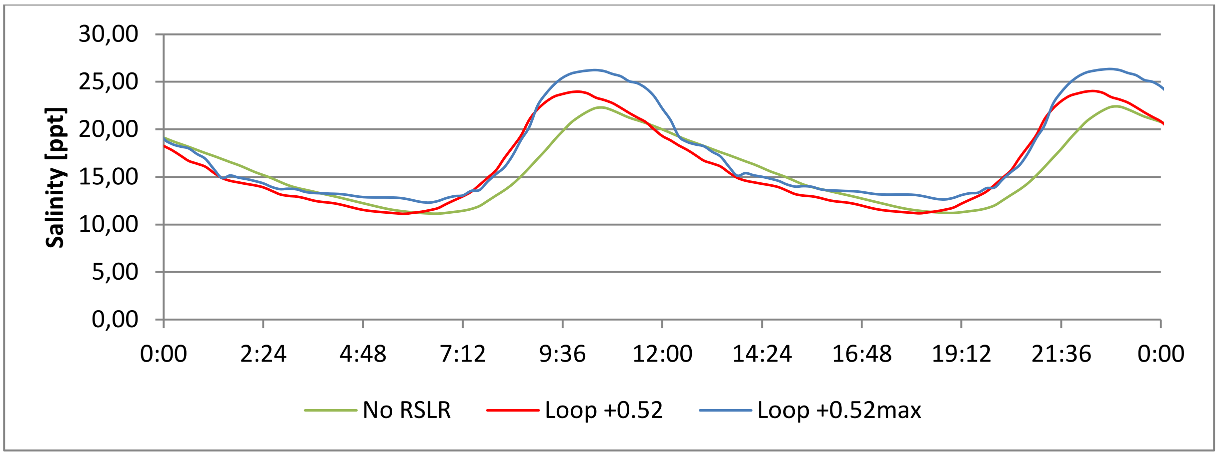

FIGURE 5.4: SALINITY LEVELS AT CTD2 WITH A 'LOOPED' OR STABLE BC.

For scenario B3 'Loop +0.52max' the model needs more time to reach the threshold of a 0.25 ppt difference between two consecutive tidal cycles. This takes approximately two weeks of simulation time. This is due to the fact that also this scenario started with the same salinity level distribution as the other two simulations shown in Figure 5.4, and thus need to adjust more to reach its equilibrium. This scenario, with its extreme water levels, shows greater impact on salinity levels in the model domain. Salinity peaks 5.6 ppt higher than in the scenario with no RSLR and extreme water levels. Upstream migration of the salt profile is now estimated to be 1.93 km and salinity maximum is found to be 12 minutes earlier than in the situation without RSLR or extended tidal range. Peaking only 12 minutes earlier seems odd, when comparing it to the scenario with only RSLR, which peaked 36 minutes earlier. As water levels are even higher in the 'Loop +0.52max' scenario, we would expect an even smaller influence of friction and subsequent earlier peak. However the water level cycle used in this third scenario has a different shape than the other two. Because of the larger tidal range, water level gradients created by the tide are now more extreme. This means peak time between scenario 3 and the other two cannot be fairly compared. The main tendency is clear however. Higher water levels at the downstream BC lead to earlier peaking of salinity, higher peaks, and a salt profile migration.

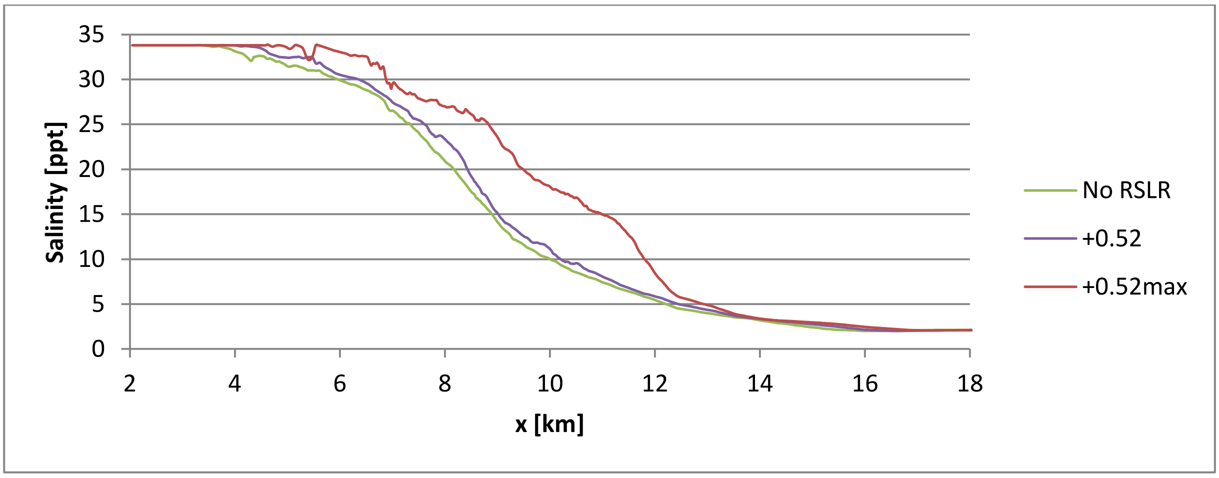

FIGURE 5.5: SALT PROFILE MIGRATION FOR SET B. THE DISTANCE 'X' IS MEASURED FROM THE RIVER MOUTH. SALINITY LEVELS ARE TAKEN FROM THE MIDDLE OF THE RIVER WHEN LEVELS WERE AT THEIR PEAK MOMENT IN TIME.

Results seem plausible as other scholars find similar results in their analyses. One study conducted in the Tamsui river in Taiwan finds the salinity profile to move by 400, 1200 and 1600 meter respectively as a response to 0.34, 1.05 and 1.40 meter sea level rise (Chen et al., 2014).

5.4.3 *Sensitivity analysis*

In the calibration process a number of factors have been calibrated: the bathymetry, roughness, eddy viscosity, eddy diffusivity and ICs. During the calibration process salinity response as a result of bathymetrical changes quickly proved significant, which is a conclusion supported by Van Ballegooyen et al. (2004). Despite this, bathymetry is not described further in the sensitivity analysis, as this is impossible to put into a single number or graph. Also sensitivity for the IC is not described, as dynamic equilibrium has been shown to be reached after only limited simulation time.

The sensitivity analysis is focused on the response of salinity levels for changes in five factors: RSLR (downstream BC) and discharge (upstream BC) in this section, and eddy viscosity, eddy diffusivity and roughness in appendix A. The results will be presented in graphs describing salinity levels at location CTD2 for various values of the discussed parameter.

Downstream BC: RSLR

Influence of RSLR on salinity levels seems to be a gradual process. Larger RSLR equals higher salinity levels at slightly earlier moments in time. This was already demonstrated in the previous section. Figure 5.6 neatly shows the impact of RSLR on the rivers' salinity levels at CTD2, as well as the rivers' longitudinal salinity profile in Figure 5.7. Finally Figure 5.8 shows the relations between RSLR and salt profile migration to be seemingly linear.

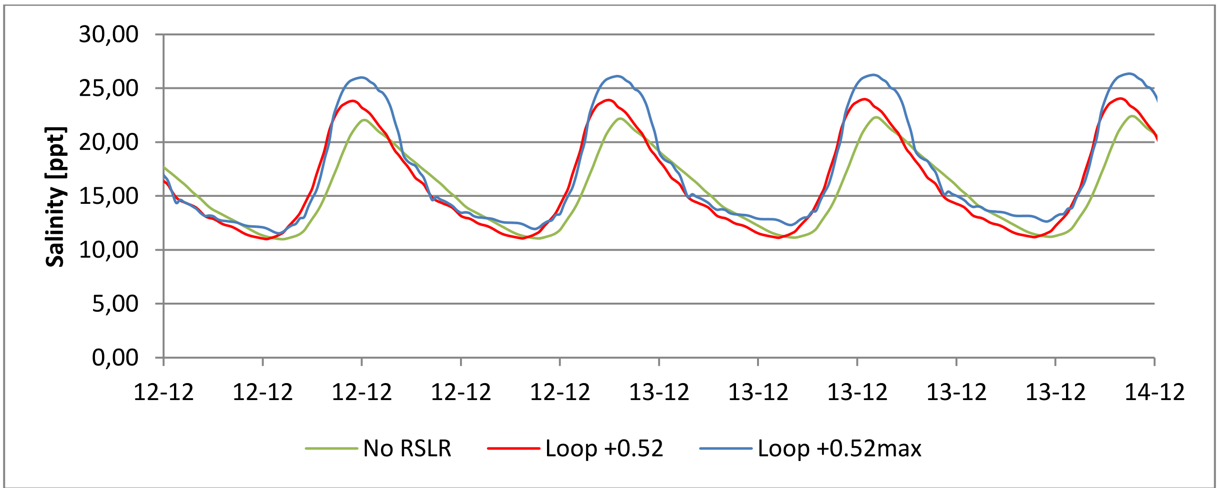

Figure 5.6: Salinity levels at CTD2 for various RSLR simulations.

In Figure 5.7 we can observe the response in salinity over the entire river. The graph shows a profile, taken at the moment of peak salinity in the middle of the river. This profile does not run completely smooth, attributable to several reasons. All data points are taken along the channel at a single moment in time close to slack tide, so water is likely to flow in many directions around this time. In addition concentrations are influenced by water from the three major overflow areas whose salinity is less directly influenced by the flow in the river, probably mixing and having an effect on the local salinity levels in specific grid cells of the model.

The salinity gradient along the channel also becomes slightly steeper for increasing RSLR, thus creating a smaller mixed zone between the salty ocean water and the fresh river water.

RSLR higher than 0.52 meter is also simulated, however results are to be looked at critically. A higher RSLR creates such high water levels in the model, that the bathymetry should actually be expanded, so to include more of the riparian zone which would at that stage also be flooded. This will be discussed in more detail in the following section.

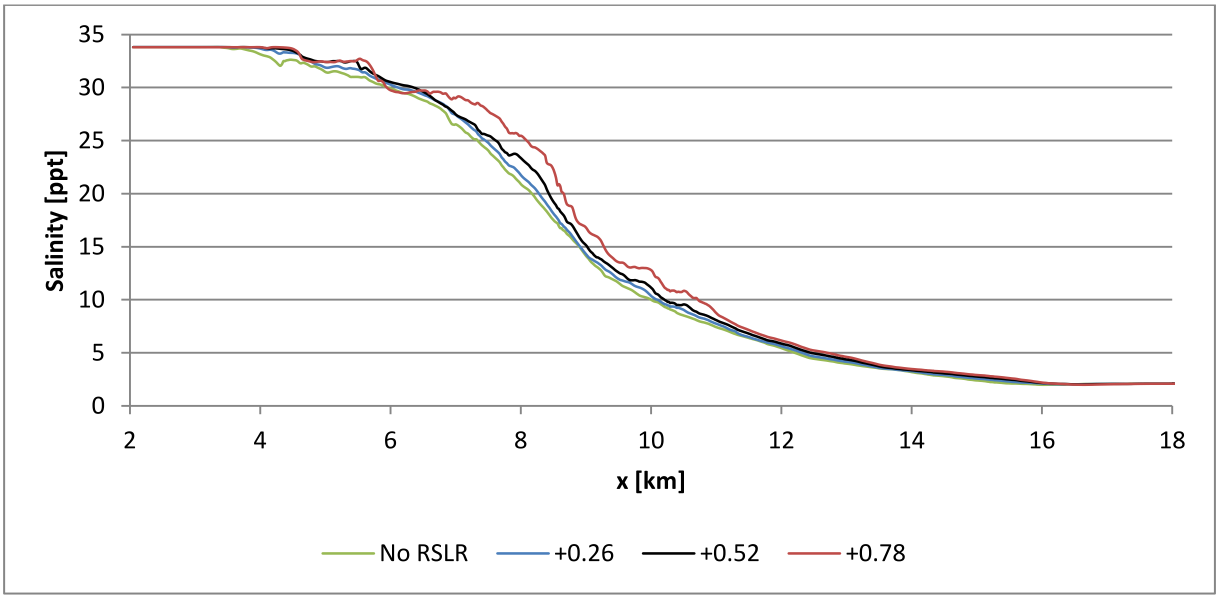

FIGURE 5.7: SALT PROFILE MIGRATION FOR VARIOUS RSLR SIMULATIONS AT THE MOMENT OF SALINITY LEVEL PEAK. THE DISTANCE IS MEASURED FROM THE RIVER MOUTH IN UPSTREAM DIRECTION.

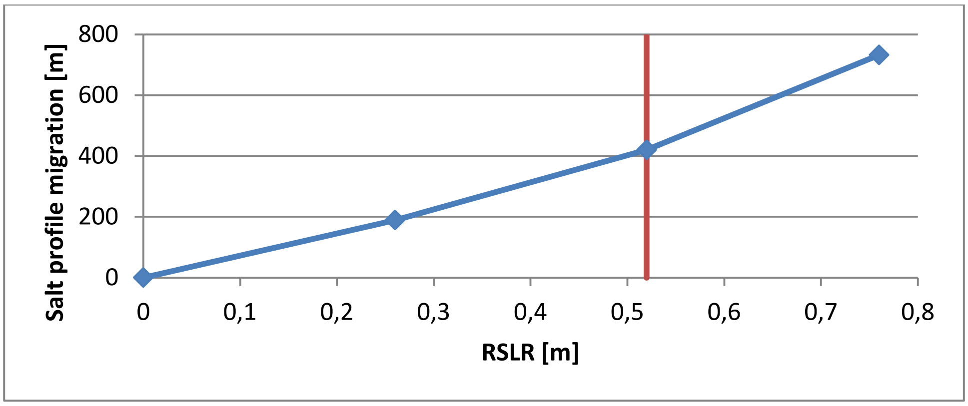

FIGURE 5.8: SALT PROFILE MIGRATION AS A FUNCTION OF RSLR AT CTD2. THE VERTICAL LINE REPRESENTS THE 0.52 M RSLR LINE, AFTER WHICH RESULTS ARE NOT CONSIDERED QUESTIONABLE.

Discharge

As we have already seen in the previous paragraph, the model seems to respond quite strongly to small changes in the discharge. Measured discharge in December was approximately 60 liters per second, which is rather limited. However the zero discharge simulation described in the results already showed a significant impact on salinity. Figure 5.9 shows model results for different upstream BC settings: 0 m^3/s, 0.06 m^3/s, 0.11 m^3/s 0.15 m^3/s, which are all constant discharges. In all cases the model started with the same salinity distribution in the model domain. The model was ran until a dynamic equilibrium was reached, in the case of 0.15 m^3/s taking about 3 weeks of simulation time.

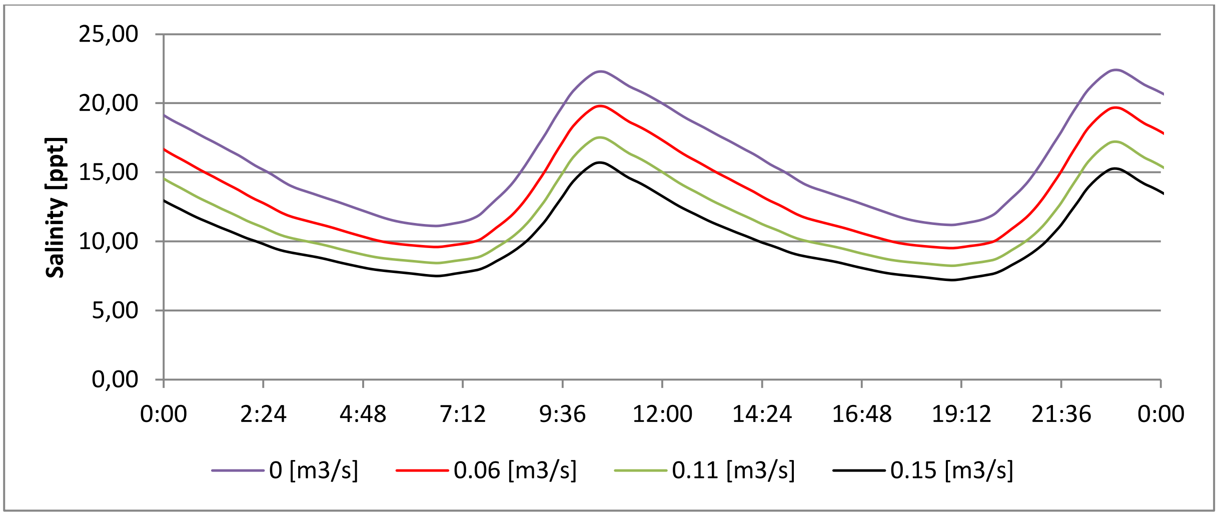

FIGURE 5.9: MODEL SENSITIVITY FOR DISCHARGE.

Influence of discharge seems to be a lot stronger than influence of RSLR. These minor adjustments to the upstream BC already show a strong impact on entire salt profile as depicted in Figure 5.10. Also in the case of increasing discharge the mixed zone, between ocean water and fresh river water, becomes smaller.

Figure 5.11 shows the relations between discharge and salt profile migration under the modeled circumstances. Similar to the relation between RSLR and salt profile migration, this also seems to be a close to linear relation for the modeled range of discharge.

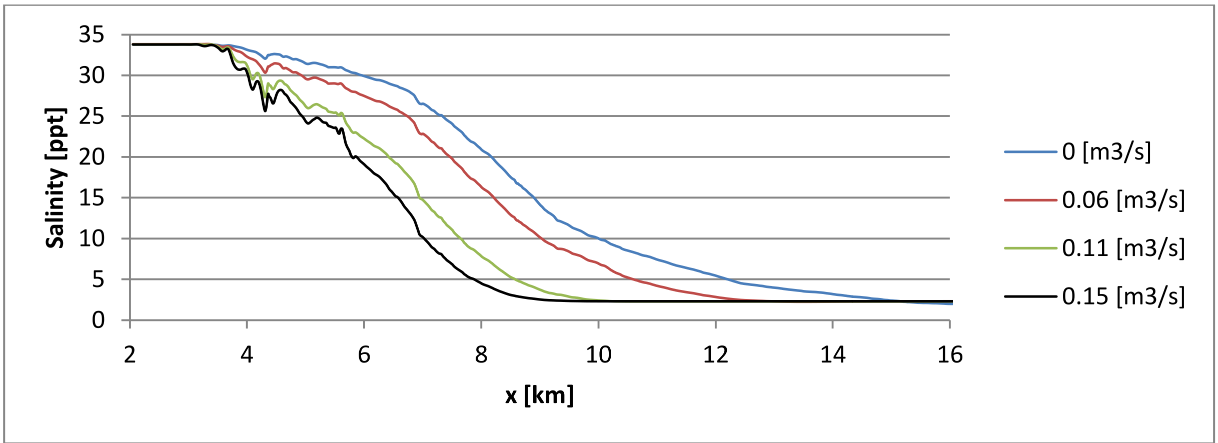

FIGURE 5.10: SALT PROFILE MIGRATION FOR VARIOUS DISCHARGE SIMULATIONS AT THE MOMENT OF SALINITY LEVEL PEAK. THE DISTANCE IS MEASURED FROM THE RIVER MOUTH IN UPSTREAM DIRECTION.

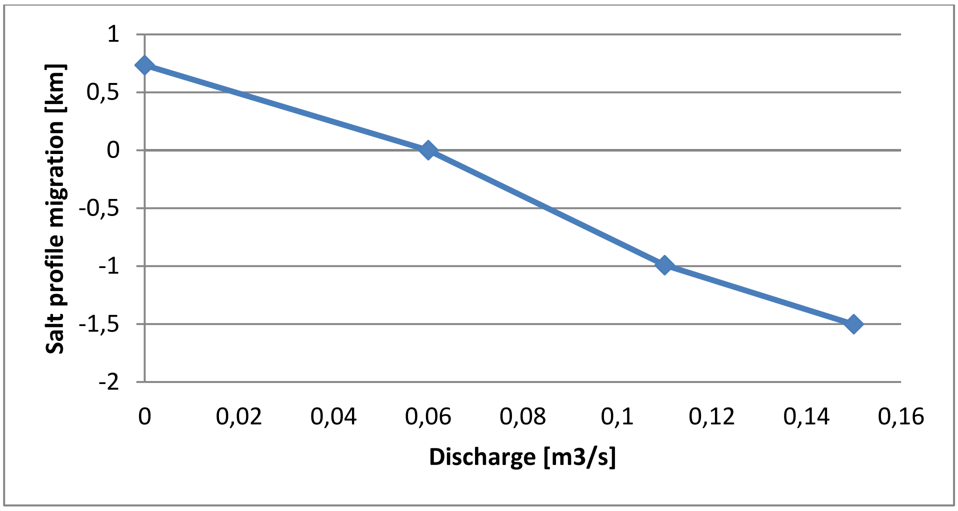

FIGURE 5.11: SALT PROFILE MIGRATION AS A FUNCTION OF DISCHARGE AT CTD2.

5.5 DISCUSSION

Obviously when modeling, there is a level of uncertainty involved. In this section the uncertainty for the model results will be discussed.

A number of factors have been neglected in the model. First of all wind has not been taken into account. During the field campaign some quite strong winds have been encountered, which have an influence on the river. However hydrodynamic results showed only very limited deviation from observed values, making it not worthwhile to introduce more data, parameters and thus uncertainty into the model.

The same reasoning explains the choice for a uniform temperature and density, as well as the absence of an evaporation demand in the model. Concerning this last process, the evaporation, it must be noted that on the longer term a clear increase in salinity was observed at all stations (see Figure 4.3). This increase is most likely due to evaporation of Heuningnes river itself, but also evaporation of Soetendaalsvlei, which was the source of inflow for Heuningnes river. Another factor which may have caused this increase in salinity is diffusion of sea water from the ocean slowly diffusing further upstream. Finally seepage from Kars river system with an unknown salinity is part of the possible explanation for the increase in salinity. Further enquiry into these issues will however not help answering the research questions posed, so have not been pursued any further in this thesis.

Calibration of the model was far from straight forward. Instead of only calibrating one value, the calibration process was finally completed by drawing from a virtually unlimited base of settings by involving the bathymetry in the calibration process. This was necessary as depth averaged velocity maps clearly indicated large flow velocity increases just upstream of CTD3, where a few 'islands' are present in the river. These islands combined with the grid which is only 5 cells wide mounted to a narrowing of the available width for the water to flow through. It then becomes the question how large of a correction to implement in these river stretches. It is difficult to estimate this, and introduces uncertainty into the model.

Also concerning the bathymetry, is the estimate for the height of the river banks. The level itself can best be described as an estimate rather than hard data. But perhaps more important is the implication the chosen level has. 1 meter AMSL upstream and 0.3 downstream.

When looking at bed level measurements taken in the three overflow areas which have been mapped manually and are located in the downstream part of the river, it can be estimated that larger scale flooding in the entire river area starts around 1 to 1.5 meter AMSL. So when 0.52 meter RSLR is added to the maximum water levels observed we will surely deal with flooding around the river. In the model, the water which would flow into the riparian zone, will be added to the water level of the river, giving an overestimation of the water level. Overestimation of the water level will again affect the salinity levels. This is also the reason why 0.52 has been used as the highest RSLR simulated. Using even higher levels for RSLR, as was done in scenario B3 'Loop +0.52max' is interesting for observing trends, but results is large uncertainties.

The model setting for eddy diffusivity has been set to 0 m^2/s. This works well for the calibrated scenario, however it is possible that diffusion will play a larger role when RSLR is introduced and also for scenarios with a higher discharge. This will however not be known without being able to calibrate or validate the model with a data set including this higher discharge and or water levels.

Another source of uncertainty is found in the non-uniform roughness. It is fairly straight forward to estimate the particular roughness level at the upstream, midstream and downstream part, as they can be linked to the observed and desired water levels. However where exactly the roughness increases along the river is impossible to determine with only 3 (and later 4) CTD observation stations, or may even be impossible altogether.

The grid build in Delft3D does not cover the complete Heuningnes river. Upstream part of the river has not been taken into account, because salt intrusion is not expected to reach this far in high concentrations. Also downstream the last 100 meters of the river was left out. This was done so that the water level gauge located at the pedestrian bridge could be used as the BC of the model. This allows for an accurate boundary condition, which is a very important forcing of the model. However at the same time it creates a problem. At outgoing tide all water flows down the river and passes the pedestrian bridge, the model boundary. When the flow reverses, it flows back into the river. However in the model all the water flowing back into the domain has a salinity of 33.8 ppt, while in the actual river some less salty water would have been in the final 100 meters between the ocean and the pedestrian bridge, which will flow back underneath the pedestrian bridge into Heuningnes river. Additional salinity is thus added in this way, however this is only limited and in the model time scale (1-2 weeks) not of significance, and was only noticed when doing a longer term (>month) run.

Finally the some accuracy is lost in translating the salinity values into the part per thousand values used by Delft3D, as discussed in sections 3.2.

6. General discussion

In the section 5.5 many issues regarding the modeling have already been discussed. This chapter will highlight some of the more important issues of the model, as well as focus on the broader issues concerning the way the research questions have been approached.

An important solution applied is the calibration of the water level referencing. The method used (described extensively in previous chapters), is one that gives good results in terms of model calibration results. It basically gives the freedom to shift the measured water levels in whatever position most fits the model outcome, as long as all water level measurements are shifted with the same correction. Tidal amplitude and peak timing are thus not influenced. The main issue with this procedure is that possibly shortcomings in for example the bathymetry or other parameters, are being compensated by this correcting of observed data. However it is the best method available, as field conditions did not allow for more accurate height referencing.

The upstream BC, the discharge, is an influence which is more significant than initially expected. However, it is not known whether all discharge measured at the boundary of the model domain, is actually flowing through the entire domain. The (referenced) water level difference measured between CTD1 and CTDx (most upstream) was too large to be explained by roughness, and is most likely caused by the river being not well connected between CTD1 and CTDx. It may very well be possible that part or all of this discharge is either evaporated or infiltrated, causing an overestimation of the discharge in the simulation. Based on the sensitivity analysis, this may have measurable impact onto salinity results.

Aside from Soetendaalsvlei, also Kars river is a tributary to Heuningnes river. At the time of the field campaign Kars river was already dry. However in winter, when Kars is also discharging, this definitely changes some of the dynamics of Heuningnes river. Impact of this is not known as no discharge data is available for Kars river, and no bathymetrical survey was doable in a dry river with the time and equipment constraints at hand. This exclusion of the Kars river domain works fine in scenarios with low water levels, so without RSLR, but becomes more concerning when RSLR is introduced to the model. A much higher water level is likely to deflect some of the water into the Kars domain at high tide, even if Kars is actually not flowing at the time. However the model did not predict ocean salinity to reach that far upstream, so for the scenarios simulated this is probably not a direct issue.

Most important limitation to the model is the limited data available for the riparian zone. For all scenarios with water levels above 1-1.5 meter there is likely to be flooding of the riparian zone, while the model does not allow for this. In many occasions for the scenarios with RSLR the high water peaks are in this grey zone, making results more uncertain.

Aside from these issues, there are also some issues concerning scales. RSLR is a process which takes place at a time scale of centuries. Aside from the sea level many things can change in this amount of time. Perhaps most importantly, the bathymetry. When looking at satellite pictures of Heuningnes river, long term changes can be easily identified. A number of oxbow lakes can be found next to the river. Also siltation plays a role when modeling changes of these time scales. The bathymetry is however assumed to be conservative in the model, which as stated will not be the case in real life. Possibly siltation will rise hand in hand with sea level, resulting in more limited RSLR, but likely more inundations as the river bed level becomes closer to the surrounding land. All these processes are very hard to predict and out of the scope of this thesis, but it is still important to be aware of these processes and not assume model simulations to show absolute truths.

Looking at the methods used in this research project, one thing is obvious. It is cheap. But cheap in a good way. Data collection was done using water level and salinity loggers, which any water institute will have available. Bathymetry was surveyed using a SONAR which costs a couple hundred euros, however this could also have been done manually if needed. Discharge was measured using a propeller, but using a piece or reed and a stopwatch gave results which were within acceptable range, making the propeller more or less redundant. The only relative expensive type of equipment used was the Trimble system which referenced the various CTD locations. Delft3D is now open source, and QGIS (also open source) works just fine for processing all spatial data. Obviously other rivers or research question may need different approaches, but from the experience of this study it seems that a lot can be done with a laptop, a brain and some help of local actors.

7. Conclusions and Recommendations

To find a suitable answer to the posed research questions an extensive field campaign was conducted in and around Heuningnes river South Africa. Two months of water level and salinity data was collected at 4 sites, 8931 depth and bed level observations were taken, and discharge was monitored during the entire campaign. Additionally secondary climate and water level data was collected at different local institutions as well as the experiences of local landowners. Based on these data a Delft3D model was build consisting of more than 7000 cells with all observed BCs implemented.

7.1 Conclusions

At an early stage of this thesis a literature study was conducted showing a number empirical relations between river parameters, and salt water intrusion. Is has however proven to be very difficult to estimate these parameters without detailed observations. The initial estimation of an intrusion at low water slack of 1.3 km, later proved to be largely underestimating the salt intrusion. Even with more detailed observations these empirical relations do not seem to be applicable to Heuningnes river.

A more robust method is to observe the conductivity at multiple points through time, as has been done during an extensive field campaign. The gathered observed data already gives answers to some parts of the questions posed. Salinity in Heuningnes river is attributable to two sources. First obvious source is the Indian Ocean, which dominates salinity levels in the downstream part of Heuningnes river. The second source, which becomes more much pronounced in summer, is the upstream inflow. As summer progresses salinity levels in the upstream part of Heuningnes increase from 1.6 ppt to over 10 ppt in about 2 months time, likely due to evaporation of the headwaters. The same process also affects the Heuningnes river itself, with evaporation leaving the same mass of salt in less water.

Concerning the distribution of salinity levels through the river under various circumstances the Delft3D model gives excellent insight. The calibrated model shows good correspondence with observed data. Allowing for reliable simulations of RSLR within limitations of the model. RSLR simulations show a clear impact in salinity levels in the river. With CTD2 as a reference location we find a 2.2 ppt increase in peak salinity resulting from a 0.52 meter RSLR. This corresponds with a 397 meter upstream push of the salt profile. In an effort to recreate a more extreme scenario, the highest water level peak recorded between 2010 and 2015 at the river mouth was applied as a BC resulting in a 5.6 ppt increase in salinity peaks, and a salt profile migration of 1.93 km. Based on these model results it seems unlikely for sea water to reach all the way into Soetendaalsvlei, however the model is not equipped to handle the associated water level heights, so more research would be needed to fully assess this question.

In addition discharge has an important impact on salinity, which shows to be larger than expected. The discharge found upstream in Heuningnes river was initially thought to be negligible, but model simulations even for this low discharge already show the impact on the downstream regions' salinity. Drawing from simulations for the sensitivity analysis and comparing the measured discharge to the same situation without discharge, resulted in a 733 meter upstream migration of the salt profile.

From a more broader perspective we can conclude that the strong influence of discharge and downstream water levels on salt intrusion have once again been confirmed. Using Delft3D we are able to see the effects on a very local, very detailed level. These simulations show clearly that salinity in Heuningnes river is likely to increase in the coming century as a result of RSLR. This will have implications for local landowners, their crops, and for nature preservation in the area. In addition to an increase in salinity, RSLR is also likely to cause more frequent inundations around Heuningnes river. When these inundations also become increasingly saline, the local practice of nature and farming may very well need adjustment in the future.

7.2 RECOMMENDATIONS

In order to prepare for the longer term future it is important to have an idea what awaits us. This study already sheds some light onto this issue. However main limitation lies within the fact that the riparian zone is not well surveyed and the model is only valid up to a limited water level. A more extended model allowing for higher water levels would give a lot more of additional information. It would allow us to see exactly which parts of the catchment would be inundated and in addition give us information on the water quality on the inundated lands. It would give the opportunity to run various downstream water level scenarios, including scenarios in which the river mouth is closed, or partially closed.

A good bathymetry of the entire area, which includes all areas below roughly +2 meter AMSL should be acquired. This could for instance be done by a LIDAR survey of the riparian area at low tide, combined with the bathymetrical data gathered in this thesis. Additional time series of water levels and salinity at various points together with discharge upstream in Heuningnes and inflow of Kars would be a good way to validate the model for winter (high flow) circumstances.

This would give local landowners and nature conservation authorities good insight in future loss of land and water quality changes which can be expected in the coming century, giving them the possibility to make constructive plans to manage their future.

8. BIBLIOGRAPHY

Bickerton, I. B. (1984). *Estuaries of the Cape Part II: Synopsis of Available Information on Individual Systems. Report No. 25: Heuningnes (CSW 19)*.

Campbell, I. C. (2009). *The Mekong: Biophysical environment of an international river basin*. Academic Press.

Cape Nature. (2005). *Wetland restoration: Nuwejaars, Heuningnes, Kars and Ratel wetland and river systems: Information status quo report and recommendations*.

Chen, W.-B., Liu, W.-C., & Hsu, M.-H. (2014). Modeling assessment of a saltwater intrusion and a transport time scale response to sea-level rise in a tidal estuary. *Environmental Fluid Mechanics*, *15*(3), 491–514. doi:10.1007/s10652-014-9367-y

Church, J. A., Clark, P. ., Cazenave, A., Gregory, J. M., Jevrejeva, S., Levermann, A., … Stammer, A. S. P. (2013). *Sea Level Change. In: Climate Change 2013: The Physical Science Basis. Contribution of Working Group I to the Fifth Assessment Report of the Intergovernmental Panel on Climate Change*. Cambridge.

Coppens, A. B. (1981). Simple equations for the speed of sound in Neptunian waters. *Journal of the Acoustical Society of America*, *69*(3), pp 862–863.

Deltares. (2011). Delft3D-FLOW User Manual.

DWAS (2011). *State of the River Report: Rivers of the Breede Water Management Area 2011*. River Health Programme.

Fischer, H. B. (1974). Discussion of "Minimum length of salt intrusion in estuaries" by B.P. Rigter, 1973. Journal Hydraul. Div. Proc. 100.

Friedrich, G., & Pohlmann, M. (2009). Long-term plankton studies at the lower Rhine/Germany. *Limnologica - Ecology and Management of Inland Waters*, *39*(1), 14–39. doi:10.1016/j.limno.2008.03.006

Ge, J., Ding, P., & Chen, C. (2011). Impacts of Deep Waterway Project on Local Circulations and Salinity in the Changjiang Estuary, China. *Coastal Engineering Proceedings*, *1*(32), 1–9. doi:10.9753/icce.v32.management.44

Haralambidou, K., Sylaios, G., & Tsihrintzis, V. a. (2010). Salt-wedge propagation in a Mediterranean micro-tidal river mouth. *Estuarine, Coastal and Shelf Science*, *90*(4), 174–184. doi:10.1016/j.ecss.2010.08.010

Harcourt-Baldwin, J.-L., & Diedericks, G. P. J. (2006). Numerical modelling and analysis of temperature controlled density currents in Tomales Bay, California. *Estuarine, Coastal and Shelf Science*, *66*(3-4), 417–428. doi:10.1016/j.ecss.2005.10.001

HiLand Associates. (2009). *Draft ESTUARY MANAGEMENT for the Heuningness Estuary*.

Hu, K., & Ding, P. (2009). The effect of deep waterway constructions on hydrodynamics and salinities in Yangtze Estuary, China. In *Journal of Coastal Research* (pp. 961–965). Retrieved from http://www.scopus.com/inward/record.url?eid=2-s2.0-78449272851&partnerID=tZOtx3y1

Kurup, G., Hamilton, D., & Patterson, J. (1998). Modelling the effect of seasonal flow variations on the position of salt wedge in a microtidal estuary. *Estuarine, Coastal and Shelf …*, 191–208. Retrieved from http://www.sciencedirect.com/science/article/pii/S0272771498903468

Lee, J. H. W., Harrison, P. J., Kuang, C., & Yin, K. (2006). Eutrophication dynamics in Hong Kong coastal waters: Physical and biological interactions. *The Environment in Asia Pacific Harbours*, 187–206.

Lewis, E. (1980). The practical salinity scale 1978 and its antecedents. *IEEE Journal of Oceanic Engineering*, *5*(1), 3–8. doi:10.1109/JOE.1980.1145448

Leyton, A. O. (2008). *Behind the pathways of mercury in the Itenez- Guapore basin, mapping the potential deposition and transformation zones*. International Institue for Geo-information Science and Earth Observation (ITC).

Mizuno, K., & Watanabe, T. (1998). Preliminary Results of in-situ XCTD / CTD Comparison Test, *54*, 373–380.

Ndungu, J., Augustijn, D. C. M., Hulscher, S. J. M. H., Kitaka, N., & Mathooko, J. (2013). Spatio-temporal variations in the trophic status of Lake Naivasha, Kenya. *Lakes and Reservoirs: Research and Management*, *18*(4), 317–328. doi:10.1111/lre.12043

Nguyen, A. D. (2008). *Salt Intrusion, Tides and Mixing in Multi-Channel Estuaries*. Taylor & Francis. doi:10.1201/9781439828342

Ocean Engineering Corporation. (2015). Single Beam Echo Sounding. Retrieved from http://www.ocean-eng.com/english/bathymetricsurvey/

OTT. (2009). Operating instructions Groundwater datalogger. Version 01-1009.

Rigter, B. P. (1973). Minimum length of salt intrusion in estuaries. *Journal of the Hydraulic Division*, 1475–1496.

Rogala, J. T. (1999). *Methodologies employed for bathymetric mapping and sediment characterization as part of the Upper Mississippi River System Navigation Feasibility Study*. U.S. Army Engineer Waterways Experiment Station.

Savenije, H. H. G. (1986). A one-dimensional model for salinity intrusion in alluvial estuaries. *Journal of Hydrology*, *85*(1-2), 87–109. doi:10.1016/0022-1694(86)90078-8

Van Ballegooyen, R., Taljaard, S., Van Niekerk, L., & Huizinga, P. (2004). Using 3D modelling to predict physico-chemical responses to variation in river inflow in smaller, stratified estuaries typical of South Africa. *Journal of Hydraulic Research*, *42*(6), 563–577. doi:10.1080/00221686.2004.9628311

Van Breemen, M. T. J. (2008). *Salt intrusion in the Selangor Estuary in Malaysia*. University of Twente.

Van den Heuvel, S. (2010). *Modeling the hydrodynamics and salinity of the Pontchartrain Basin*. *Delft University of Technology*.

Van Os, A.G., and Abraham, G. (1990). Density currents and salt intrusion. Delft.

Vaughan, E. G., Crutcher, J. M., & Chairman, V. (2011). *Bathymetric Survey of the Guadalupe River*. Austin.

APPENDIX A: MODEL SENSITIVITY FOR ROUGHNESS AND TURBULENCE PARAMETERS

ROUGHNESS

Change in salinity as a result of a change of roughness of +10 $m^{1/2}/s$ is 2.0 ppt at the peaks of the graph. Similar values are found for -10 $m^{1/2}/s$. The either +5 $m^{1/2}/s$ or -5 $m^{1/2}/s$ scenarios show a maximum increase and decrease or 1.0 ppt also around the peaks and troughs, see Figure A.1.

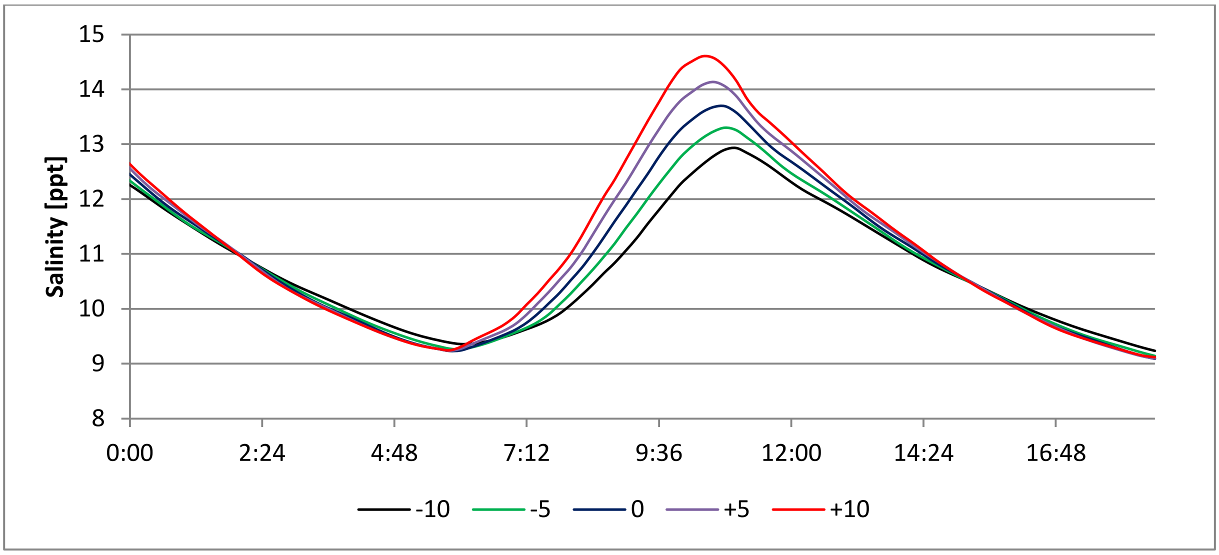

FIGURE A.1: MODEL SENSITIVITY FOR ROUGHNESS AT CTD2.

EDDY VISCOSITY

In determining the sensitivity of the salinity for the eddy viscosity parameter, simulations with eddy viscosity between 0 m^2/s and 10 m^2/s have been executed. This is the advised range for smaller scale simulations (1-10 m^2/s) (Deltares, 2011), with the 0 m^2/s simulation added. Salinity and eddy viscosity have negative relation. A lower eddy viscosity produces a larger salinity value. This can also be traced back to water levels where it can be observed that the tidal range throughout the entire river increases for a decreasing eddy viscosity. Maximum decrease in salinity when comparing the calibrated value of 1 m^2/s with a simulation using 10 m^2/s is 1.4 ppt.

When approaching zero viscosity, salinity increases over the full tidal cycle. Water levels do not explain this increase in salinity, as they do not show an increase for every time-step. There thus seems to be a noticeable eddy driven salt transport.

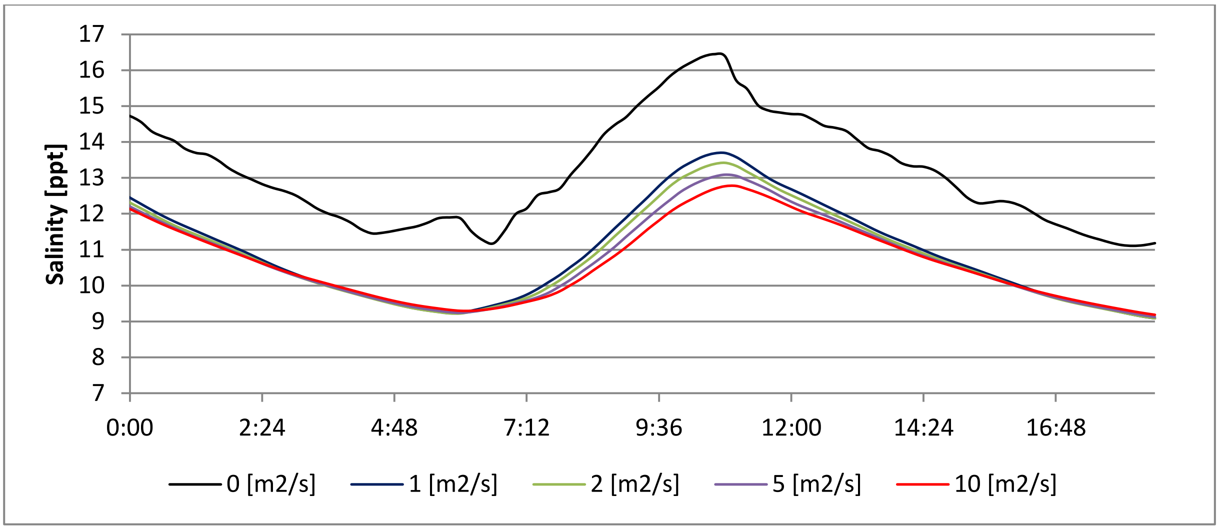

FIGURE A.2: MODEL SENSITIVITY FOR EDDY VISCOSITY AT CTD2.

EDDY DIFFUSIVITY

The range of values used for eddy diffusivity is also based on the Delft3D-FLOW User Manual (Deltares, 2011), which subscribes to use an eddy diffusivity between 1 m^2/s and 10 m^2/s. Additionally 0 m^2/s was added, as this was the calibrated value.

In the results of the various eddy diffusivity simulations a number of processes can be identified. First we see a clear divergence in salinity values. For increasing values of eddy diffusivity, salinity increases over the entire tidal cycle. Salt is thus transported from downstream by means of diffusion which of course then increases over time as salt continues to diffuse from downstream into the more upstream region. Another process which can be identified most clearly at the first few tidal cycles is the more damped amplitude of the salinity graph.

Influence of the eddy diffusivity is relative large compared to the eddy viscosity and roughness. Largest increase in salinity can be seen when comparing 0 m^2/s and 10 m^2/s, as modeled salinity increases 6.5 ppt.

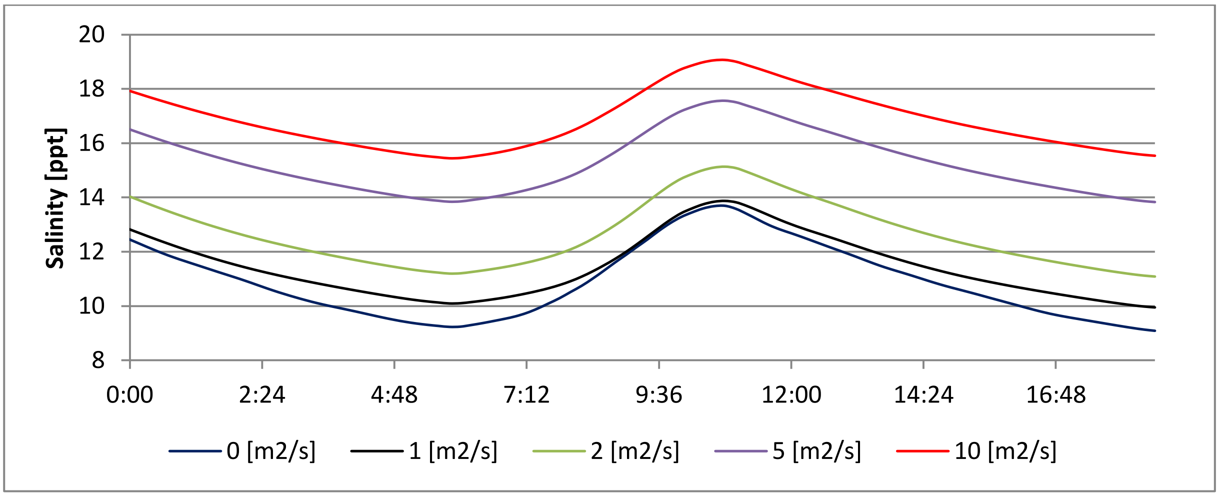

FIGURE A.3: MODEL SENSITIVITY FOR EDDY DIFFUSIVITY AT CTD2.

APPENDIX B: HEUNINGNES RIVER BATHYMETRY

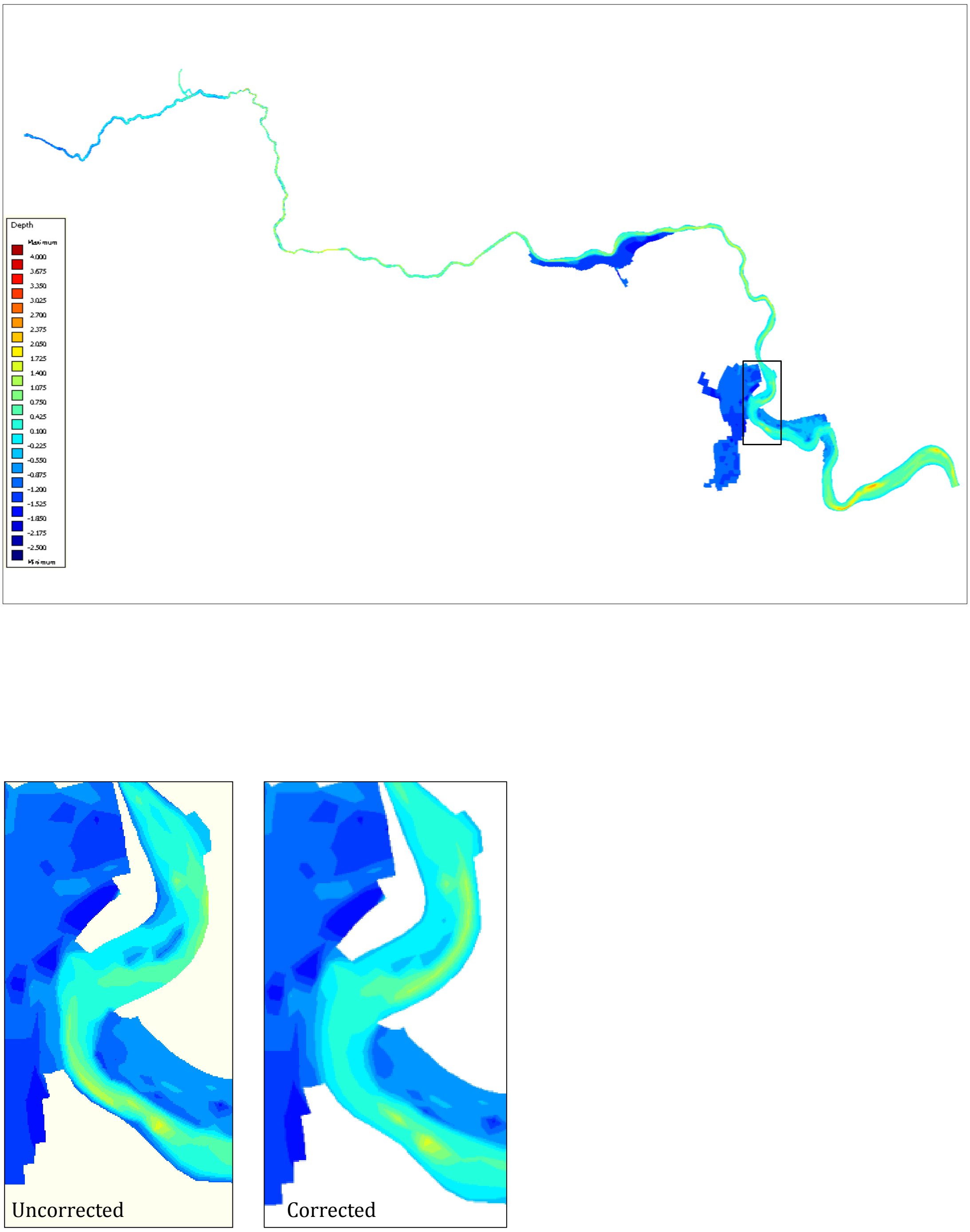

FIGURE C.1: RIVER BATHYMETRY WITH HIGHLIGHTED CALIBRATED AREA.

APPENDIX C: WATER LEVEL AND SALINITY DATA

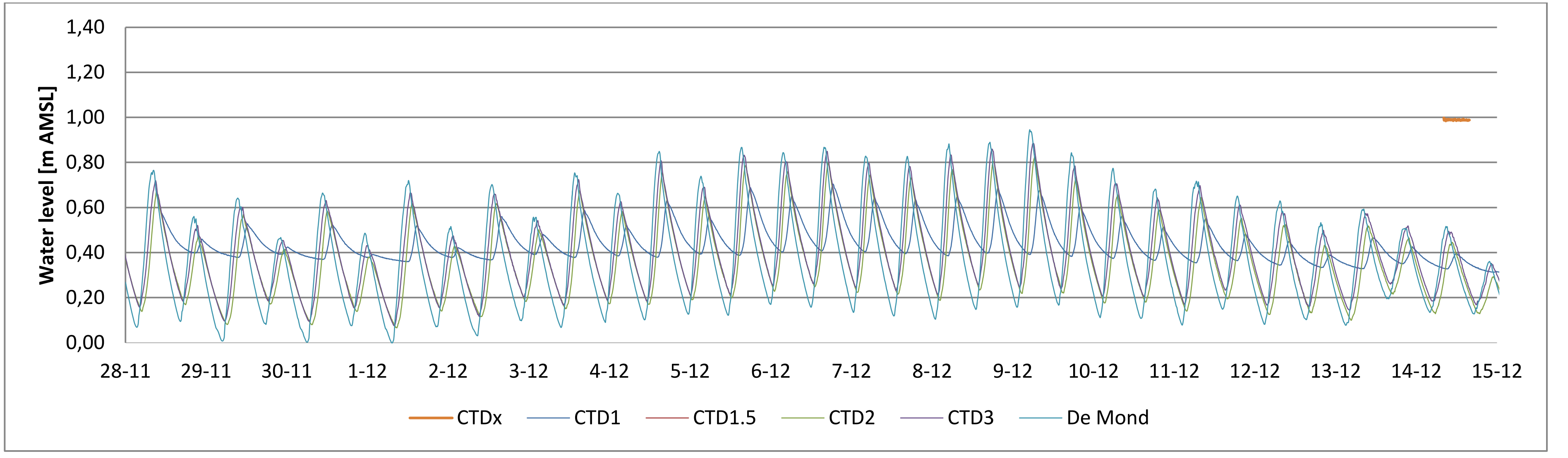

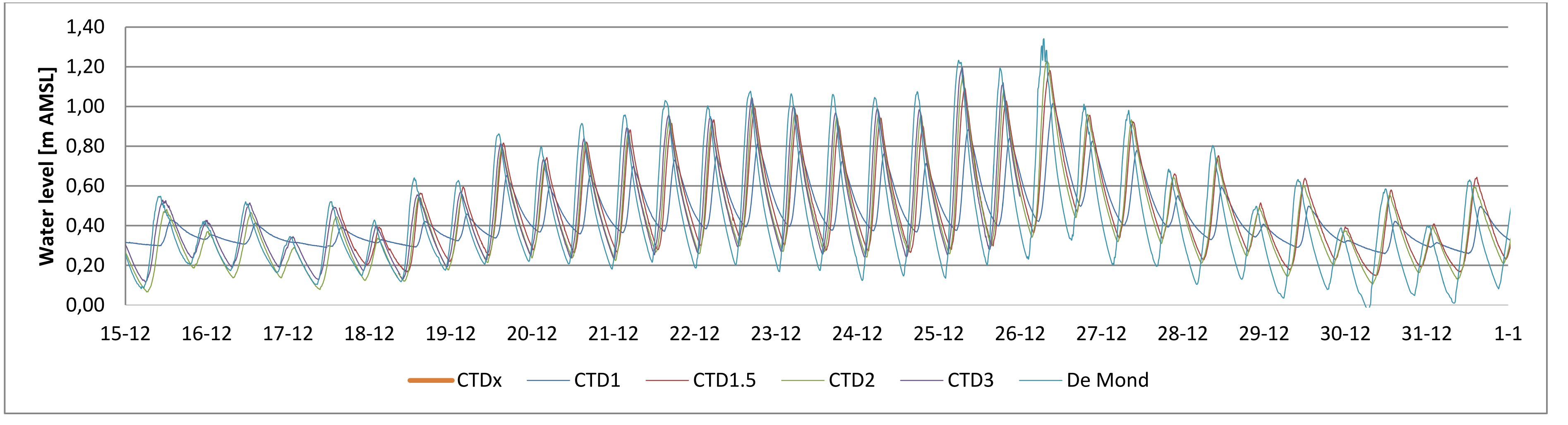

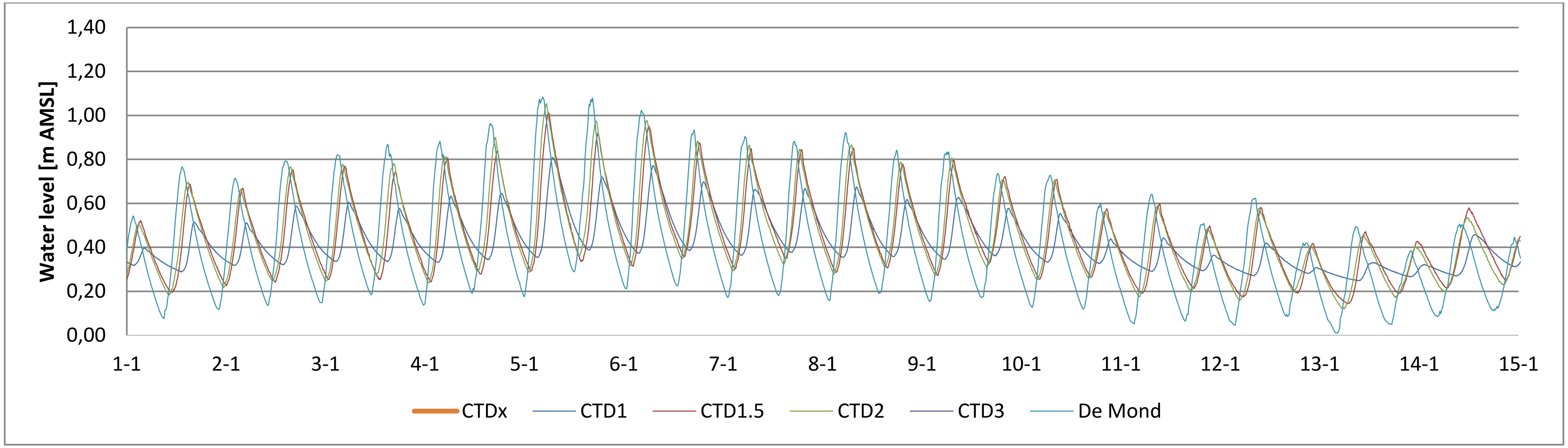

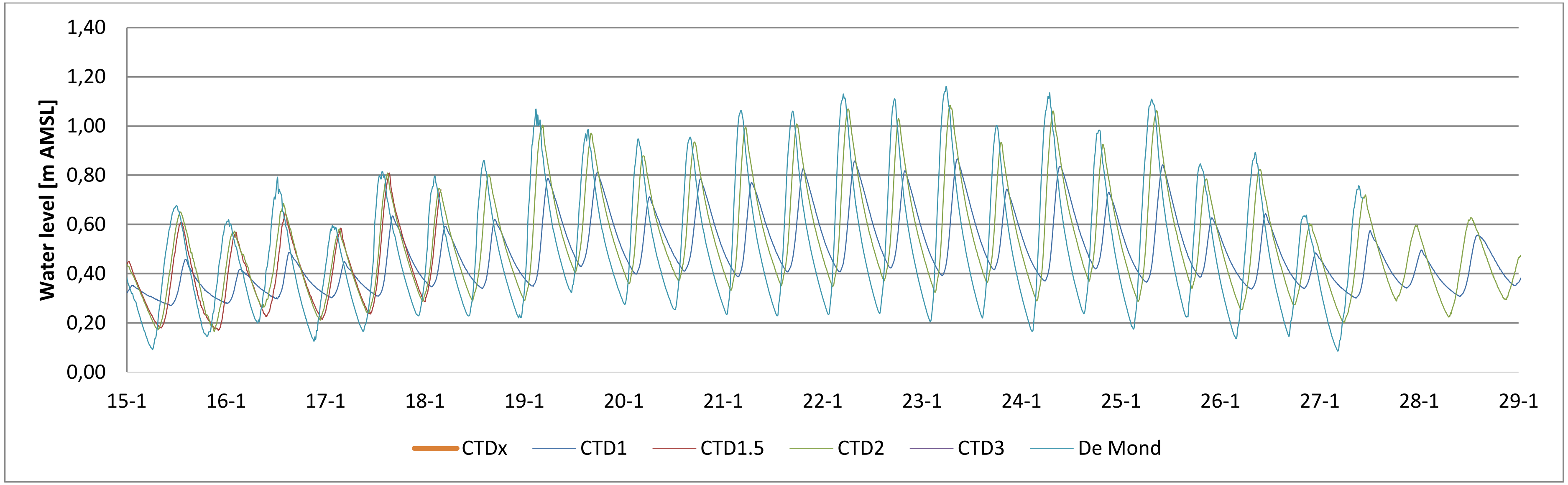

FIGURE B.1: WATER LEVELS OBSERVED AT CTD STATIONS.

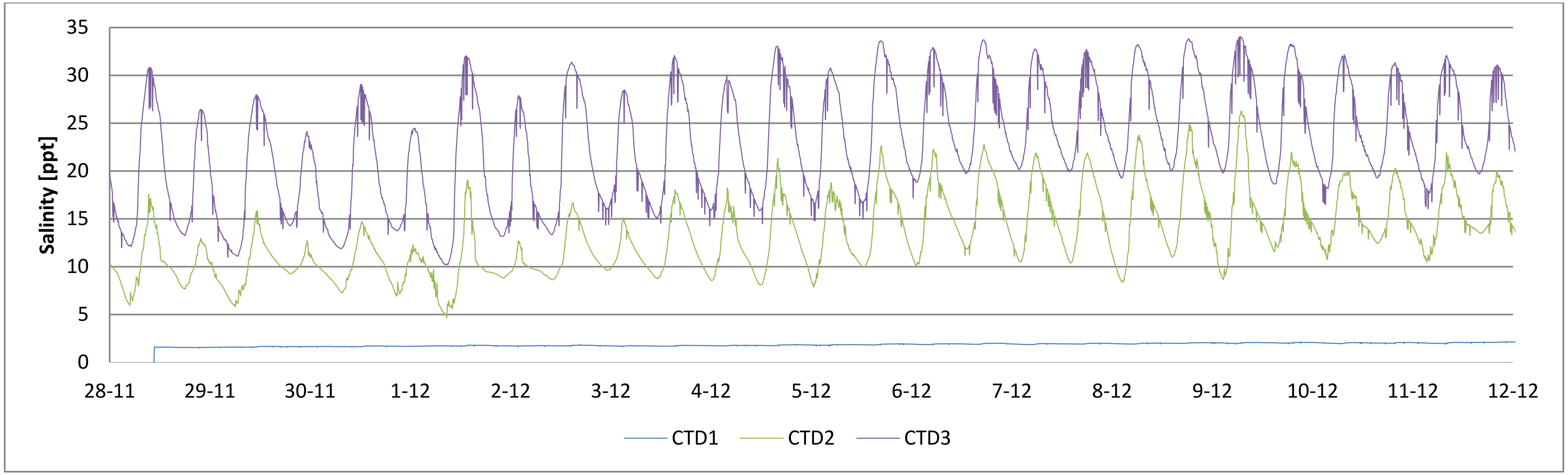

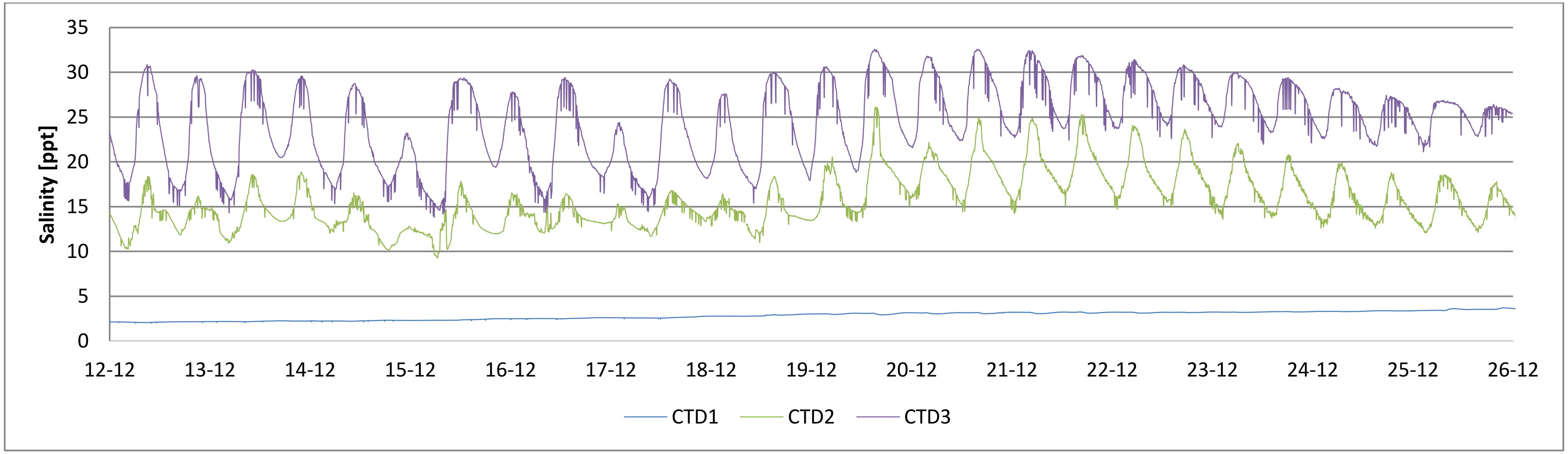

FIGURE B.2: SALINITY LEVELS OBSERVED AT CTD STATIONS.

Appendix D: Wind direction and wind speed forecasts

Table D.1: Wind speed and direction forecasts (source: Windguru.cz, GFS 27 model).

Date	**Wind speed [m/s]**								**Wind direction**							
	02h	05h	08h	11h	14h	17h	20h	23h	02h	05h	08h	11h	14h	17h	20h	23h
30.11.2014	6	6	6	4	4	2	4	4	E	E	ENE	E	SE		WSW	WSW
01.12.2014	4	4	4	5	6	7	7	7	WSW	WSW	SW	SW	SW	SSW	S	SSE
02.12.2014	8	8	9	9	10	10	10	10	SSE	SE	SE	SE	ESE	ESE	ESE	ESE
03.12.2014	10	10	10	10	9	9	9	8	ESE	ESE	ESE	E	ESE	ESE	ESE	ESE
04.12.2014	7	5	5	6	7	6	6	5	ESE	ESE	ESE	SE	SE	SE	SE	ESE
05.12.2014	5	5	6	6	8	8	7	7	E	ESE	ESE	E	ESE	ESE	E	E
06.12.2014	7	7	7	8	9	10	9	8	E	E	E	E	ESE	ESE	E	E
07.12.2014	8	8	8	8	9	8	6	6	E	E	E	E	ESE	ESE	ESE	ESE
08.12.2014	7	6	6	5	5	5	4	3	ESE	E	E	E	ESE	E	E	ENE
09.12.2014	1	7	8	9	9	8	6	4		W	W	W	WSW	SW	SW	SW
10.12.2014	3	3	3	5	6	6	5	4	SW		SSE	SE	SE	SE	ESE	E
11.12.2014	4	4	4	4	5	5	4	4	E	E	E	ESE	SE	S	SW	WSW
12.12.2014	7	8	9	9	9	8	5	3	WSW	W	WSW	WSW	SW	SW	SSW	
13.12.2014	2	4	5	6	6	6	4	2		E	ENE	E	ESE	SE	ESE	
14.12.2014	2	3	4	4	6	6	5	4		SSW	SW	WSW	SW	SSW	SSW	SSW
15.12.2014	2	4	4	4	6	6	5	4		SSE	SE	SE	SE	SE	ESE	ESE
16.12.2014	3	3	3	3	5	5	2	1	ESE			SE	SSE	SSE		
17.12.2014	1	2	3	3	4	4	4	4				ESE	SE	S	SSW	WSW
18.12.2014	4	4	4	5	7	7	4	2	W	W	W	WSW	SW	SSW	SSW	
19.12.2014	2	2	2	4	6	7	7	6				SW	SW	WSW	WSW	W
20.12.2014	6	6	6	7	8	8	6	6	W	W	W	W	WSW	WSW	WSW	W
21.12.2014	5	6	8	11	12	11	8	4	W	W	W	W	W	W	W	WSW

22.12.2014	2	1	1	2	4	4	4	4					S	SSW	WSW	W
23.12.2014	5	5	6	8	10	11	9	7	W	WNW	WNW	W	WSW	WSW	WSW	W
24.12.2014	6	6	6	7	9	11	11	10	W	W	W	W	WSW	WSW	W	W
25.12.2014	10	11	12	14	14	12	10	7	WNW	WNW	WNW	WNW	W	WSW	WSW	WSW
26.12.2014	5	4	4	4	5	7	6	7	WSW	SSW	S	SSE	SE	SE	ESE	E
27.12.2014	6	7	7	6	7	7	7	7	ESE	ESE	ESE	SE	SE	SE	SE	SE
28.12.2014	6	6	6	6	7	7	7	7	ESE	ESE	ESE	ESE	ESE	ESE	ESE	ESE
29.12.2014	6	6	7	8	9	8	7	7	ESE	E	E	E	ESE	ESE	ESE	ESE
30.12.2014	7	6	6	7	8	8	7	7	ESE	ESE	ESE	SE	SE	ESE	ESE	ESE
31.12.2014	7	7	8	8	9	10	8	7	E	ESE	ESE	ESE	E	E	E	E
01.01.2015	5	4	2	2	6	6	5	3	E	ENE			SW	SW	SSW	
02.01.2015	2	3	2	4	6	5	4	3				SW	SW	SW	SW	W
03.01.2015	4	5	6	7	10	11	9	8	W	WNW	WNW	W	WSW	WSW	WSW	W
04.01.2015	8	8	7	7	8	11	10	10	W	W	W	W	WSW	WSW	W	WNW
05.01.2015	9	9	9	11	11	12	10	9	WNW	WNW	WNW	W	W	W	W	WSW
06.01.2015	8	7	5	4	5	5	5	5	WSW	WSW	WSW	SW	S	SSE	ESE	E
07.01.2015	6	6	7	7	7	6	4	3	E	ENE	ENE	E	ESE	ESE	ESE	
08.01.2015	2	3	4	6	7	7	5	4			SW	SW	SSW	SSW	S	SSE
09.01.2015	4	4	5	7	8	9	8	7	SE	ESE	ESE	ESE	ESE	ESE	E	E
10.01.2015	7	6	4	4	6	6	4	3	E	E	E	SSE	S	S	S	
11.01.2015	2	3	2	3	5	6	5	5		SSE			SE	SE	ESE	ENE
12.01.2015	4	3	1	3	7	8	6	4	ENE				SW	WSW	WSW	WSW
13.01.2015	3	4	4	9	9	9	9	10		W	SSE	SE	ESE	ESE	ESE	E
14.01.2015	10	9	9	9	10	10	10	9	E	E	E	E	E	E	E	ENE
15.01.2015	6	3	4	8	14	17	15	9	ENE		WSW	W	WSW	W	W	W
16.01.2015	8	13	13	11	11	10	7	4	NW	WSW	WSW	WSW	WSW	WSW	SW	SW
17.01.2015	3	1	1	1	5	5	3	2					SSE	S		
18.01.2015	2	3	3	7	9	7	6	4			WNW	WSW	SSW	SSW	S	S
19.01.2015	4	4	5	7	8	8	8	7	SSE	SE	ESE	ESE	ESE	ESE	ESE	E
20.01.2015	8	8	10	11	11	8	8	6	E	E	E	E	E	ESE	ESE	ESE

21.01.2015	5	5	7	9	9	9	9	8	E	E	ESE	E	E	ESE	E	E
22.01.2015	8	8	7	7	7	7	6	5	E	ENE	E	E	ESE	ESE	ESE	ESE
23.01.2015	6	4	5	7	7	7	5	4	ESE	E	E	E	ESE	SE	ESE	E
24.01.2015	5	5	7	7	7	3	8	10	E	E	ENE	ENE	ESE	SE	WSW	W
25.01.2015	7	6	7	6	8	9	7	3	W	W	W	WSW	WSW	WSW	WSW	W
26.01.2015	2	3	4	6	7	6	5	4			W	WSW	SW	SW	SSW	S
27.01.2015	4	4	4	5	6	7	6	5	S	S	S	SSE	SE	SE	ESE	ESE
28.01.2015	5	5	7	8	9	11	11	10	E	E	E	E	ESE	E	E	ENE
29.01.2015	9	9	8	9	9	7	4	3	ENE	ENE	ENE	E	E	ESE	E	ENE
30.01.2015	2	5	9	10	12	12	11	6		WSW	W	WSW	WSW	WSW	W	W
31.01.2015	5	8	9	8	8	8	5	2	WNW	W	WSW	SW	SW	SW	SSW	